Warsaw macro-micro model and random walk method for calculating the fusion probability of superheavy elements

Aleksander Augustyn

Michał Kowal, Tomasz Cap, Krystyna Siwek-Wilczyńska

NATIONAL CENTRE FOR NUCLEAR RESEARCH
ŚWIERK

Graduate Physics Seminar
26 October 2023

Superheavy elements

- Only man-made
- Z>103 (transactinides)
- Produced in nuclear reactions:
  - Cold fusion
  - Hot fusion

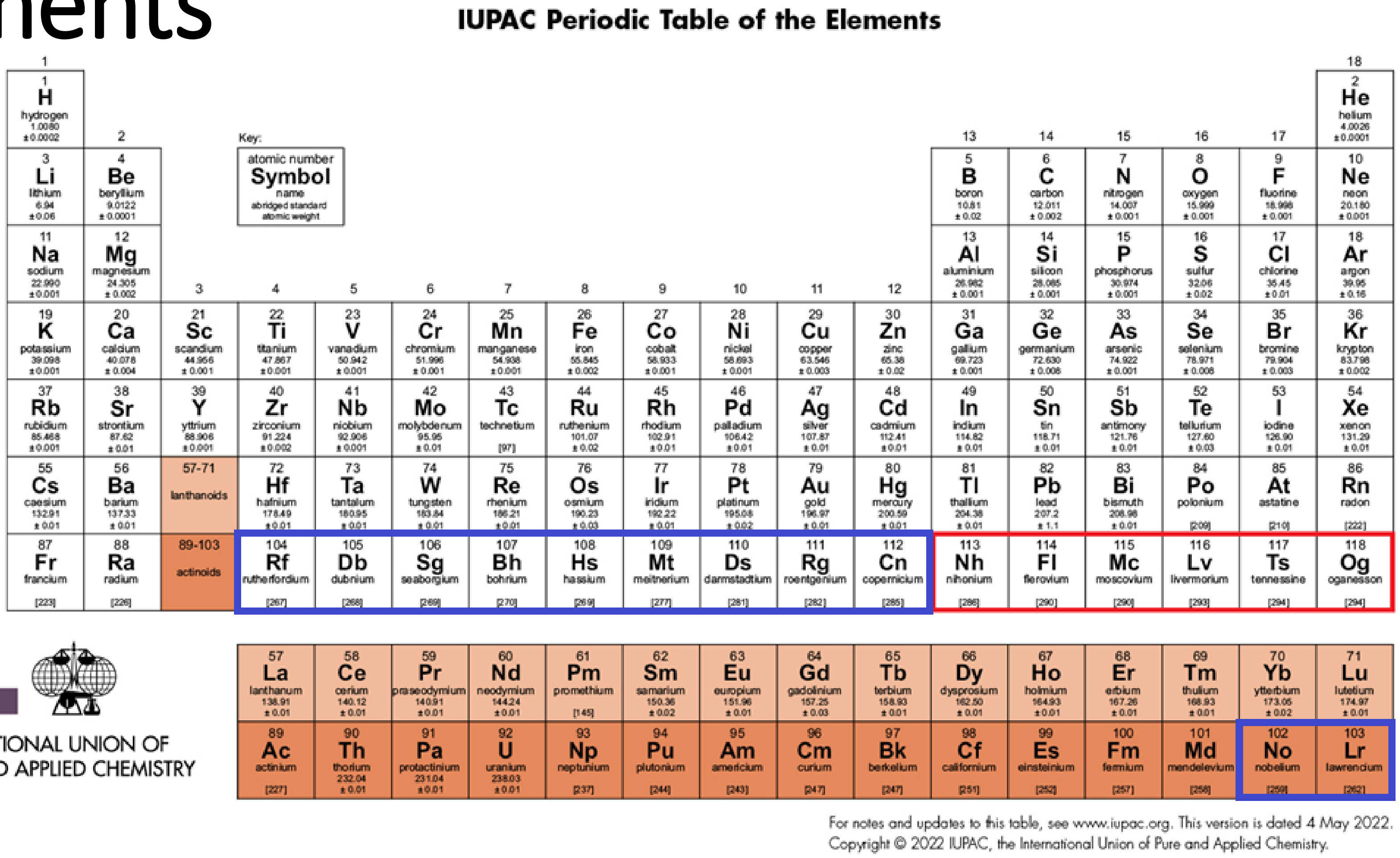

INTERNATIONAL UNION OF PURE AND APPLIED CHEMISTRY

NARODOWE CENTRUM BADAŃ JĄDROWYCH ŚWIERK

Superheavy elements

Oganessian, Yu. (2006). Synthesis and decay properties of superheavy elements. Pure and Applied Chemistry - PURE APPL CHEM. 78. 889-904. 10.1351/pac200678050889.

- Only man-made
- Z>103 (transactinides)
- Produced in nuclear reactions:
  - Cold fusion
  - Hot fusion
- Expensive process:
  - Target/Projectile production
  - Length of irradiation

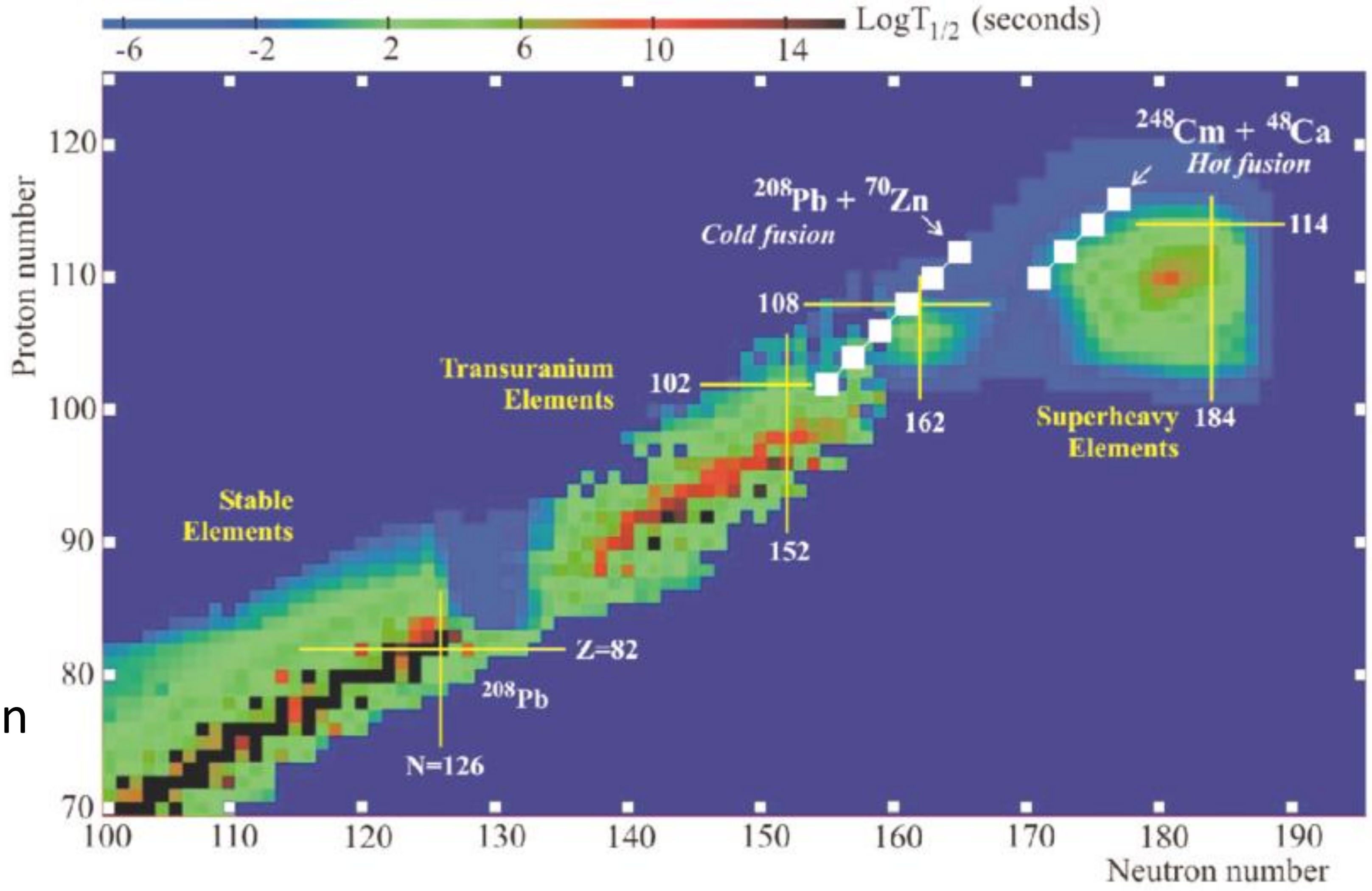

Cold and hot fusion

- $E^* \approx$ 10-20 MeV
- Compound system is only weakly heated and is cooled down via emission of just one or two neutrons
- Magic nuclei as targets (spherical shapes)
- Projectiles heavier than ^{40}Ar

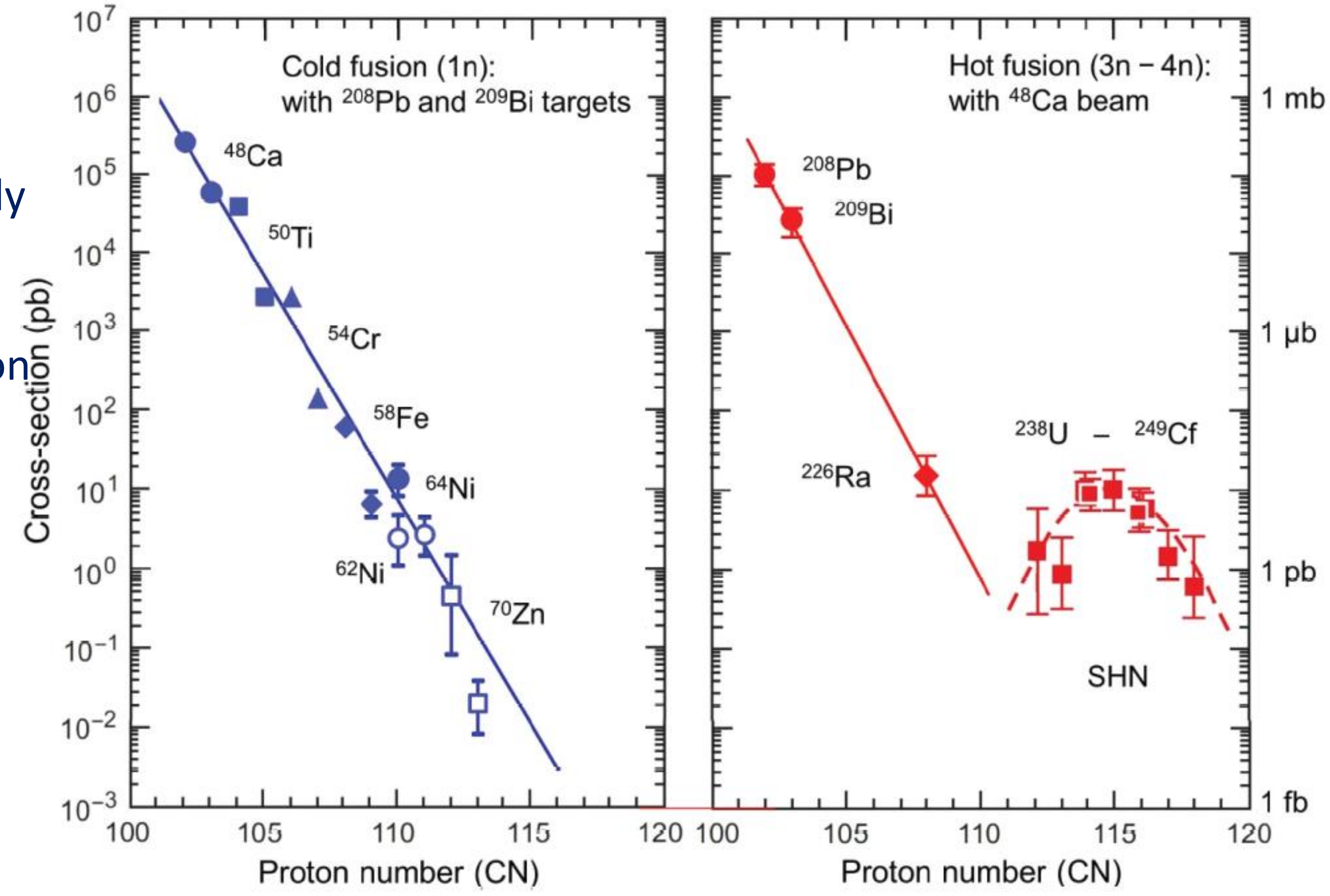

Sigurd Hofmann, Sergey N. Dmitriev, Claes Fahlander, Jacklyn M. Gates, James B. Roberto and Hideyuki Sakai
Report of the 2017 Joint Working Group of IUPAC and IUPAP, Pure Appl. Chem. 2020; 92(9): 1387–1446

- E^* = 30-40 MeV
- Compound nucleus is quite excited (most often emits 3 neutrons)
- Well-deformed radioactive actinides (Act.) targets
- Doubly magic projectile ^{48}Ca
- Attempts of going beyond the reactions Act. + ^{48}Ca by using heavier projectiles (like ^{50}Ti, ^{54}Cr, ^{58}Fe, ^{64}Ni) gave no results so far.
- Heavier actinides with Z>98 too short-lived to be used as targets

Motivation

- Experiments require theory to determine the optimal reactions and bombarding energies
- A way to calculate P_{fus} would be very helpful in the search for the new elements 119 and 120
- We wanted to use the micro-macro model with the inclusion of rotational energy and a random walk method on potential energy surfaces (PES) to calculate the probability of fusion, while describing the fusion process
- The model is first tested on cold fusion reactions with near spherical projectiles: $^{48}Ca+^{208}Pb$, $^{50}Ti+^{208}Pb$ and $^{54}Cr+^{208}Pb$

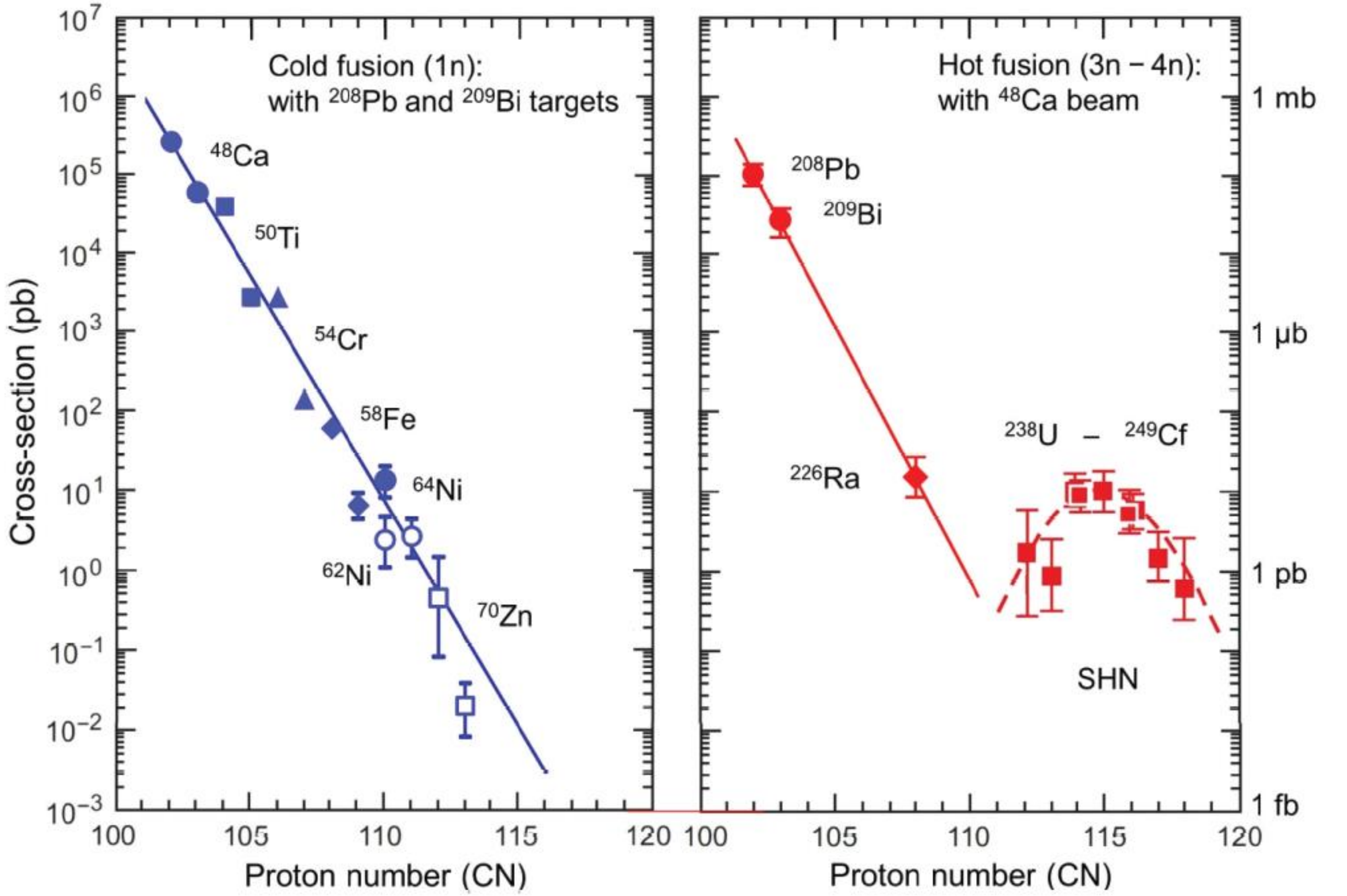

Sigurd Hofmann, Sergey N. Dmitriev, Claes Fahlander, Jacklyn M. Gates, James B. Roberto and Hideyuki Sakai
Report of the 2017 Joint Working Group of IUPAC and IUPAP, Pure Appl. Chem. 2020; 92(9): 1387–1446

FbD (Fusion-by-Diffusion) model

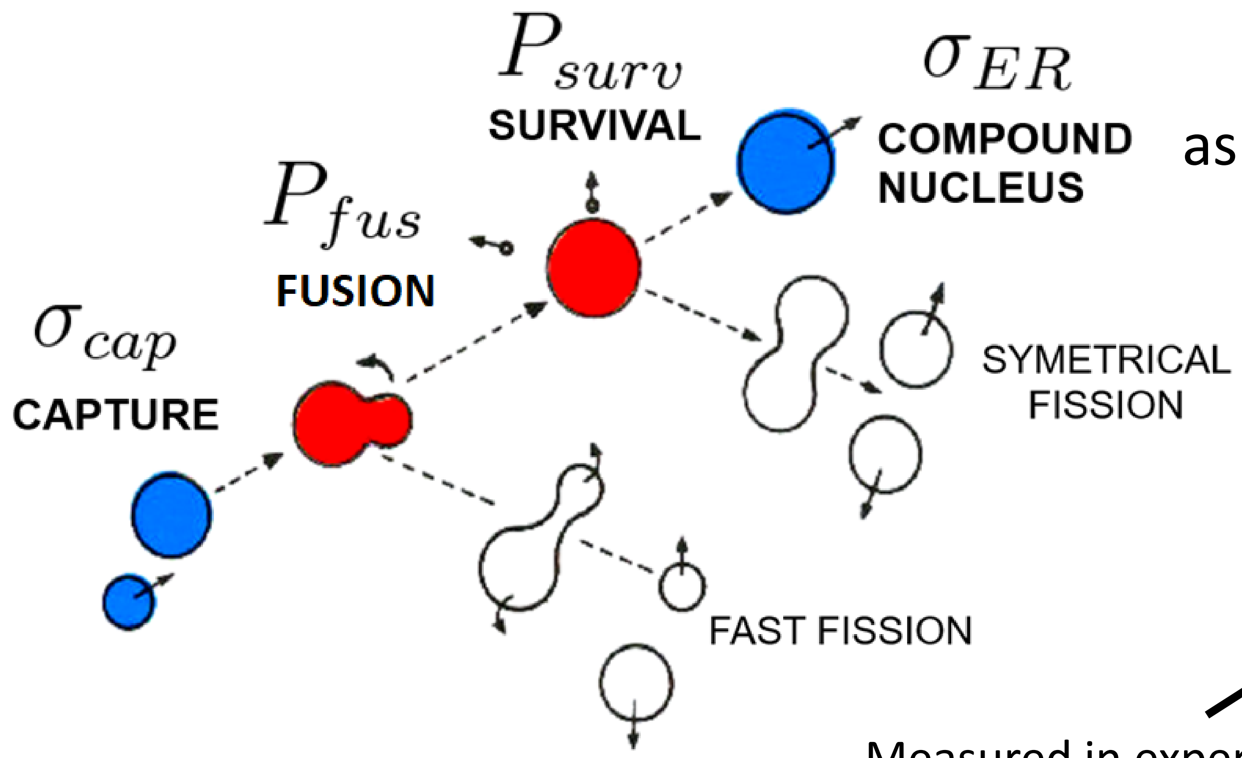

Synthesis of SHN can be described as a **3** step process, due to the different timescales of the particular reaction stages:

$$\sigma_{ER} = \sigma_{cap} \; P_{fus} \; P_{surv}$$

σ_{cap}: Measured in experiments, can be calculated using various models ← **Diffused barrier formula (Entrance channel barrier is given by a Gaussian distribution)**

P_{fus}: Not measured directly, difficult to calculate ← **Smoluchowski Diffusion Equation, Random Walk**

P_{surv}: Well established theory and formulas Monte Carlo Statistical model *Psurv* << 1 ← **masses, fission barriers, deformations from Warsaw Micro-Macro model**

W. J. Świątecki, K. Siwek-Wilczyńska, J. Wilczyński, **PRC 2005**
T. Cap et al., **PRC 2011**
K. Siwek-Wilczyńska et al. **PRC 2012**
T. Cap et al., **PRC 2013**
K. Siwek-Wilczyńska et al. **PRC 2019**

Capture cross section σ_{cap}

- The entrance channel barrier is described by a distribution that can be approximated by a Gaussian function
- The formula for the capture cross section is derived by folding the Gaussian barrier distribution with the classical expression for the fusion cross section

$$\sigma_{cap} = \pi R^2 \frac{\omega}{E_{c.m.}\sqrt{2\pi}} \left[X\sqrt{\pi}(1 + \mathrm{erf}(X)) + \exp(-X^2) \right] = $$
$$= \pi \lambda\!\!\!^{-}{}^2 (2l_{max} + 1)^2, \quad \text{where } X = \frac{E_{c.m.} - B_0}{\omega\sqrt{2}}$$

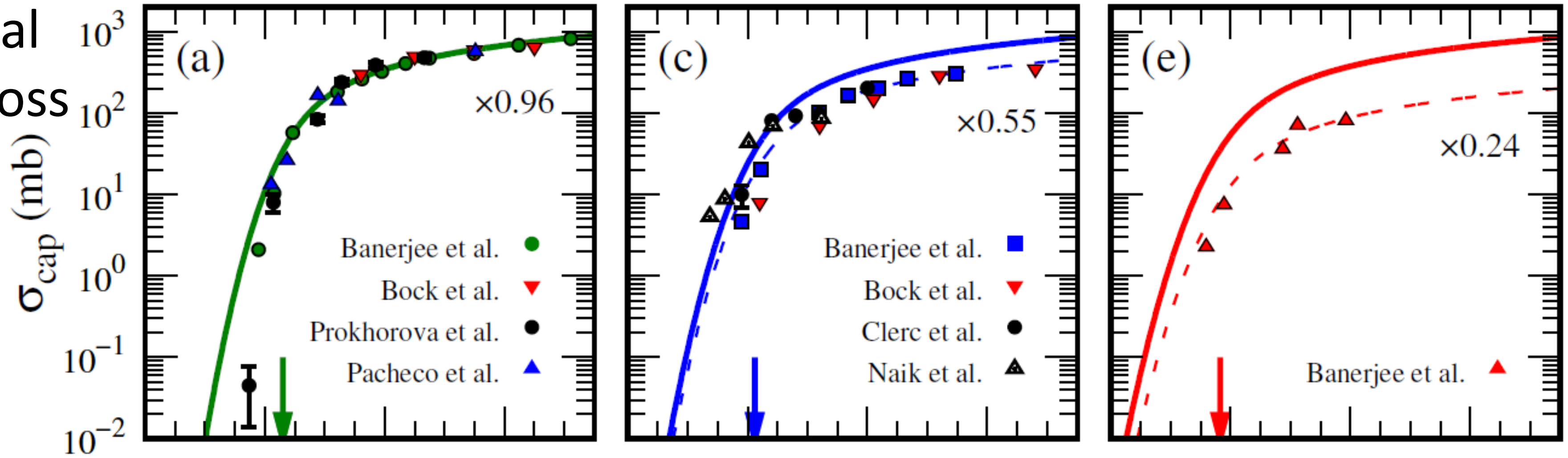

T. Cap, M. Kowal, and K. Siwek-Wilczyńska, Phys. Rev. C **105**, L051601 (2022)

NARODOWE CENTRUM BADAŃ JĄDROWYCH ŚWIERK

P_{fus} in experiment

Mechanisms Suppressing Superheavy Element Yields in Cold Fusion Reactions
Banerjee *et al.*, PRL 122, 232503 (2019)

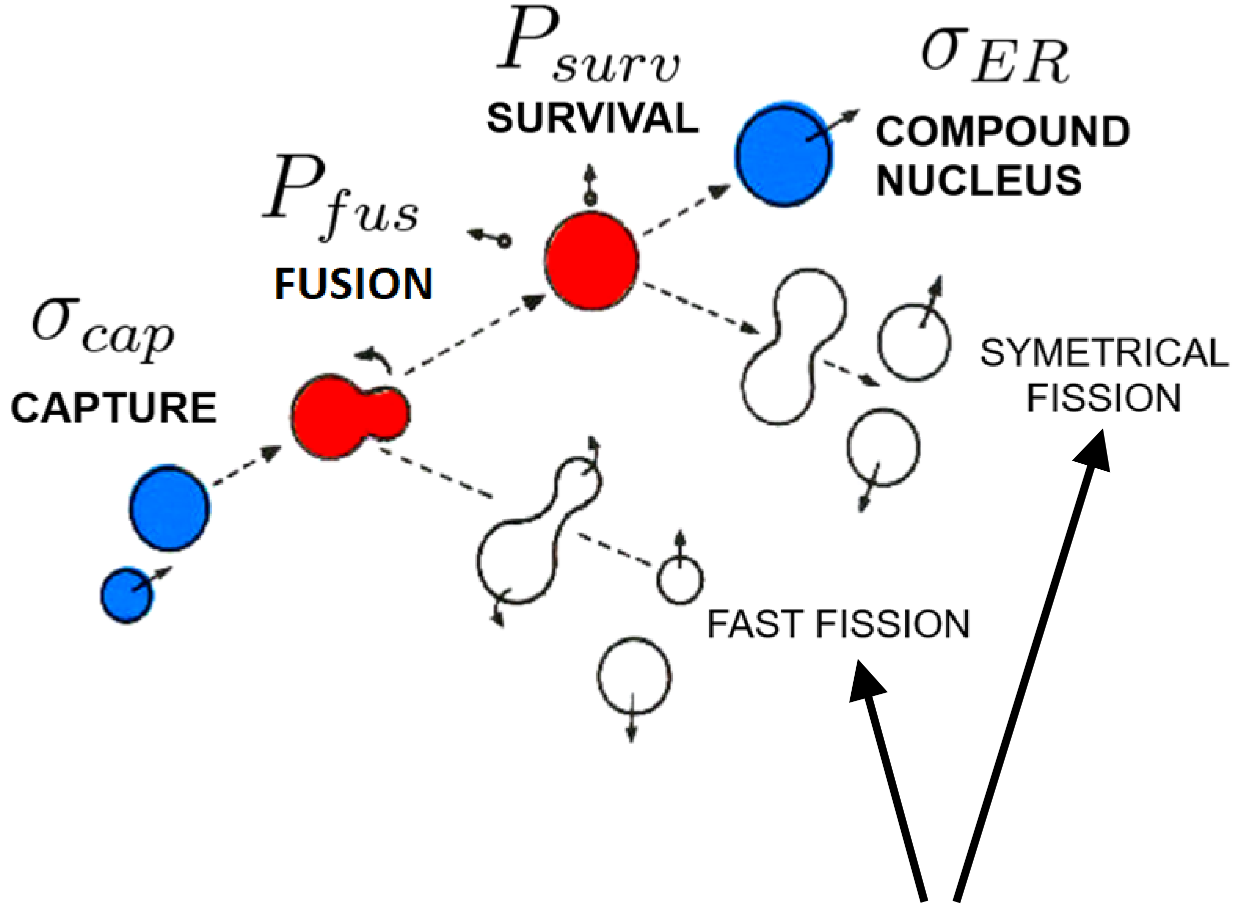

measured in the experiment

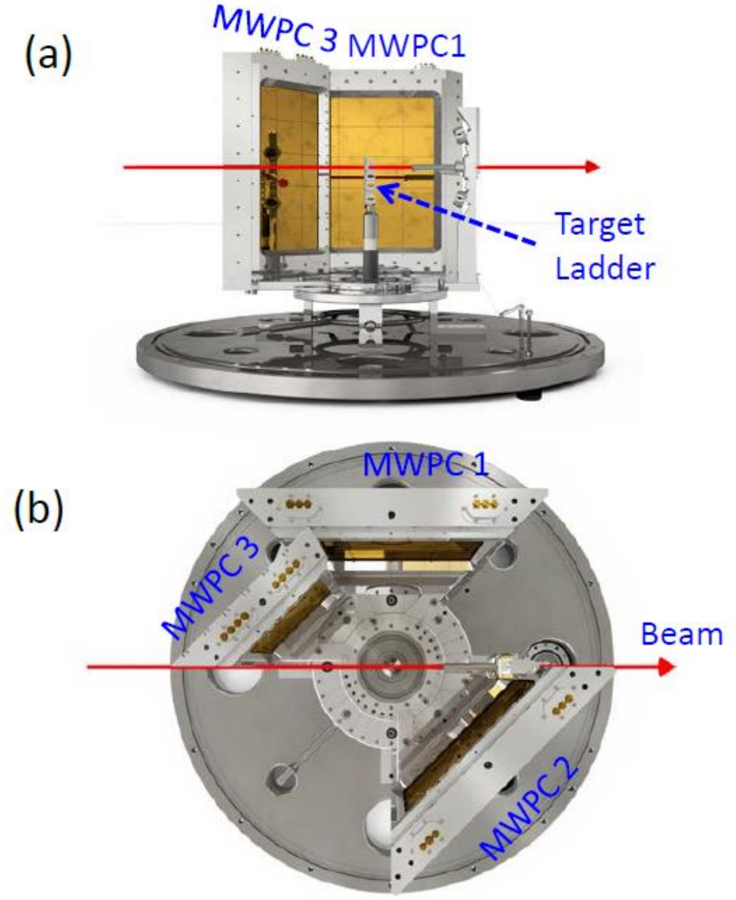

P_{fus} in experiment

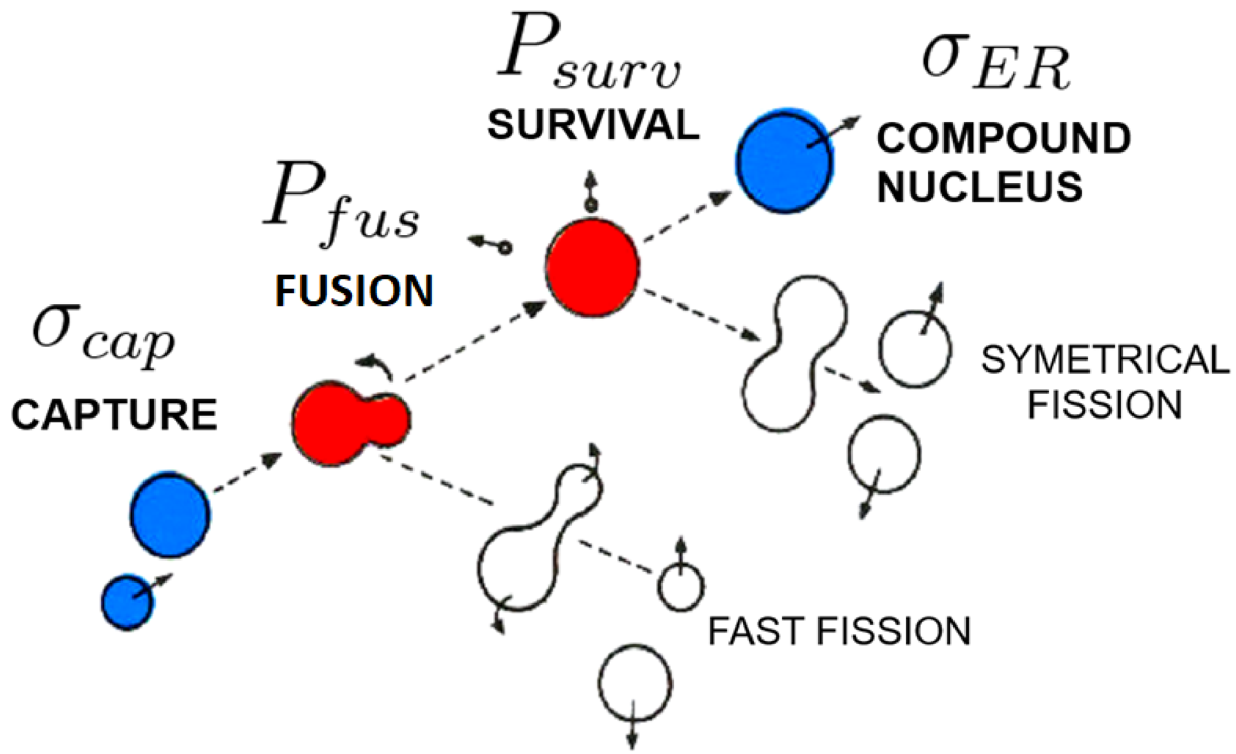

Mechanisms Suppressing Superheavy Element Yields in Cold Fusion Reactions
Banerjee *et al.*, PRL 122, 232503 (2019)

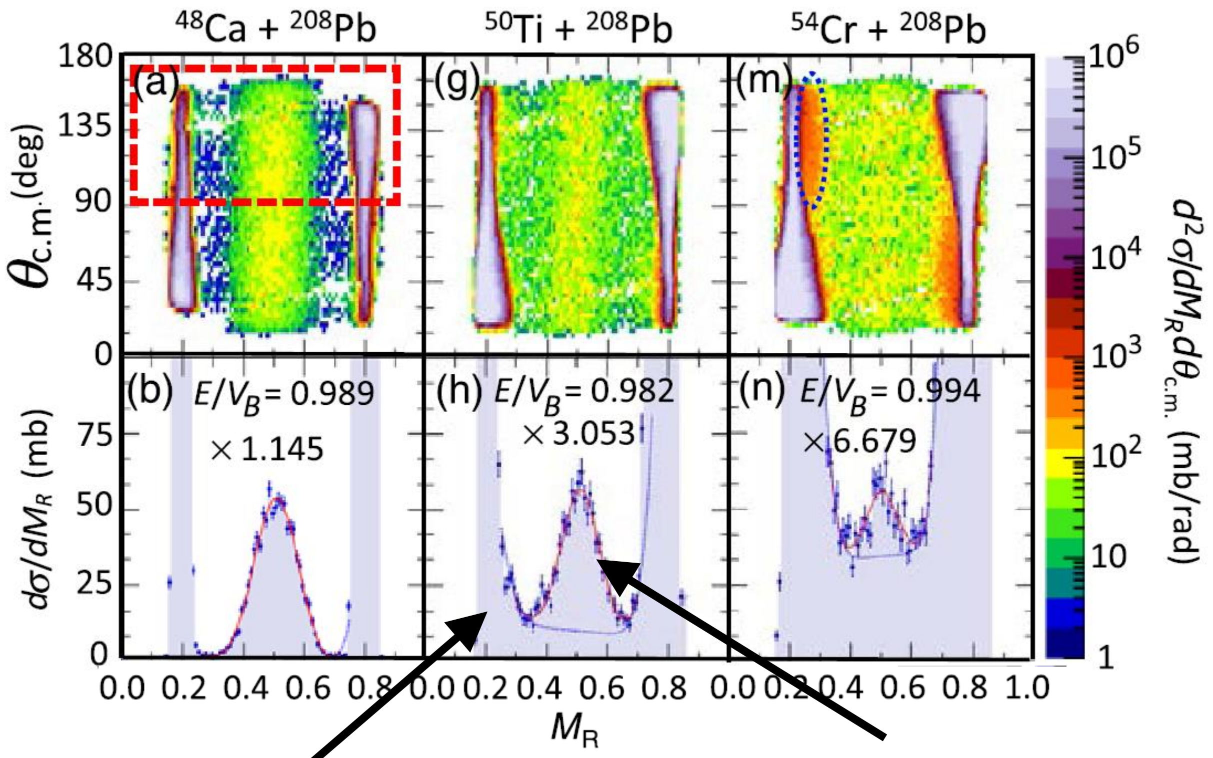

Fast Fission cross section

Mass ratio, Symmetric split: $M_R = 0.5$

Fusion-Fission cross section (symmetrical fission)

P_{fus} can be experimentally estimated:

$$P_{sym} = \frac{\textbf{Fusion–Fission cross section}}{\textbf{Capture cross section}}$$

Banerjee et al., PRL 122, 232503 (2019)

Reactions:

$^{48}Ca + ^{208}Pb \rightarrow ^{256}No^*$

$^{50}Ti + ^{208}Pb \rightarrow ^{258}Rf^*$

$^{54}Cr + ^{208}Pb \rightarrow ^{262}Sg^*$

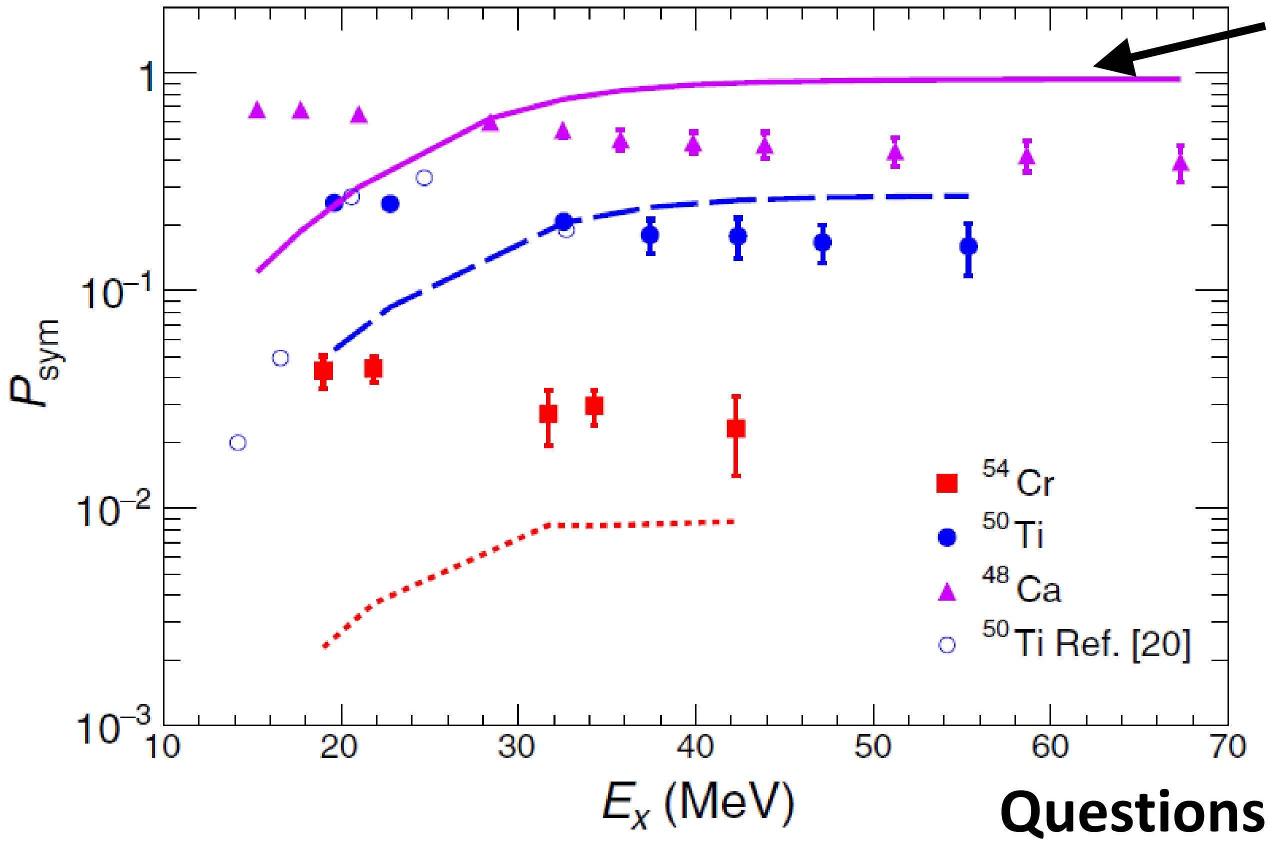

Diffusion model calculations by V. Zagrebaev and W. Greiner PRC 78, 034610 (2008).

The experimental trends are different than the model predictions for all 3 reactions.

The conclusion was that diffusion is not the main mechanism responsible for the synthesis of SHN.

Upper limit for fusion probability

Excitation energy

Questions:

Can the diffusion approach (FbD) describe the experimental results?

What is the fusion mechanism?

P_{fus} in Fusion by Diffusion

1D motion approximation
The system must overcome an internal barrier ***H*** to fuse.

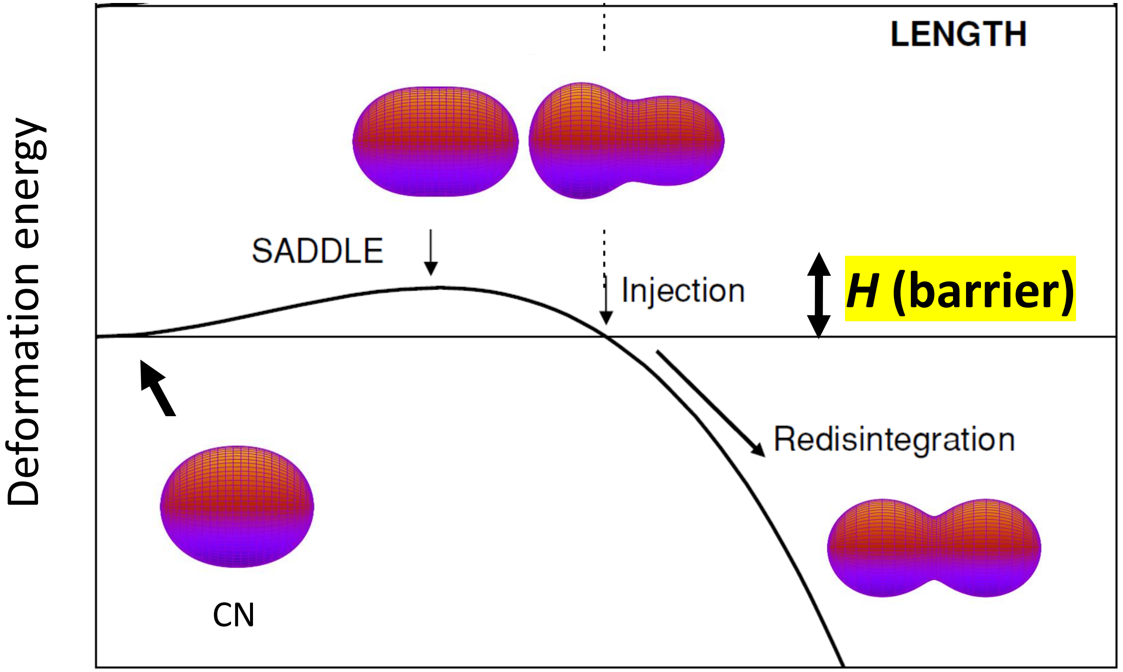

L is the effective elongation (along the fusion path)

P_{fus} is calculated by solving
1D Smoluchowski Diffusion Equation

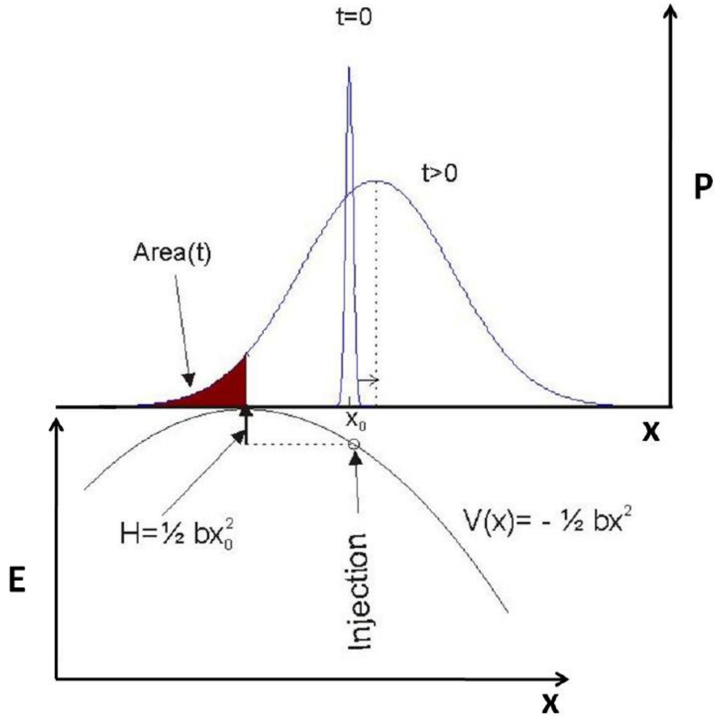

$$P_{fus}(l) = \frac{1}{2}\left(1 - \mathrm{erf}\left(\sqrt{\frac{H(l)}{T}}\right)\right) \text{ when } L_{inj} \geq L_{saddle}$$

H(l) – the function of angular momentum and bombarding energy
T – the temperature depends on available energy

NARODOWE CENTRUM BADAŃ JĄDROWYCH ŚWIERK

Fusion probability from FbD model

- Only takes into account the macroscopic binding energy
- Doesn't describe the fusion process
- Can the random walk method be better?

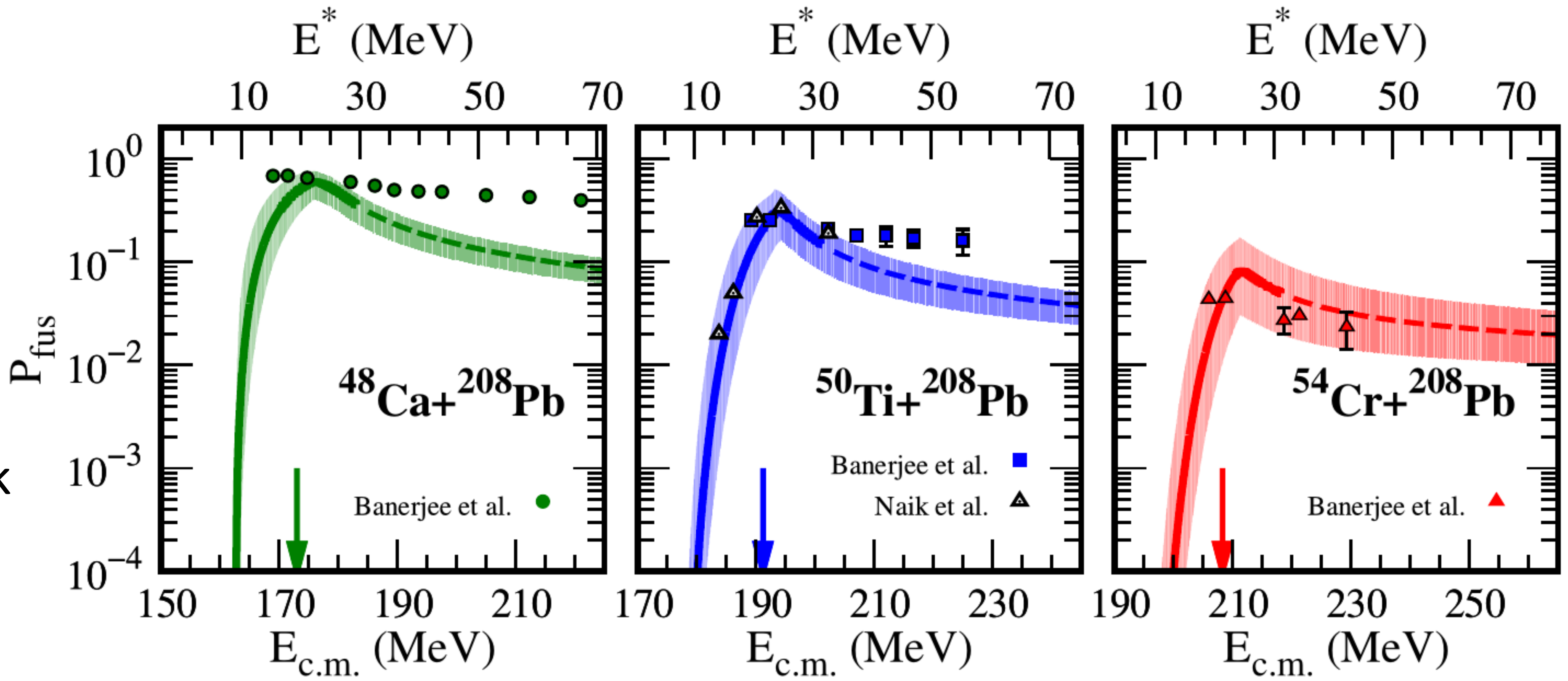

T. Cap, M. Kowal, and K. Siwek-Wilczyńska, Phys. Rev. C **105**, L051601 (2022)

Binding/Potential energy in SHE

- Macroscopic (liquid drop) and microscopic (shell effects) energy
- Shell effects responsible for superdeformed minimum in actinides
- SHE exist thanks to the shell effects creating the ground state (often deformed)
- The model needs to account for both energies

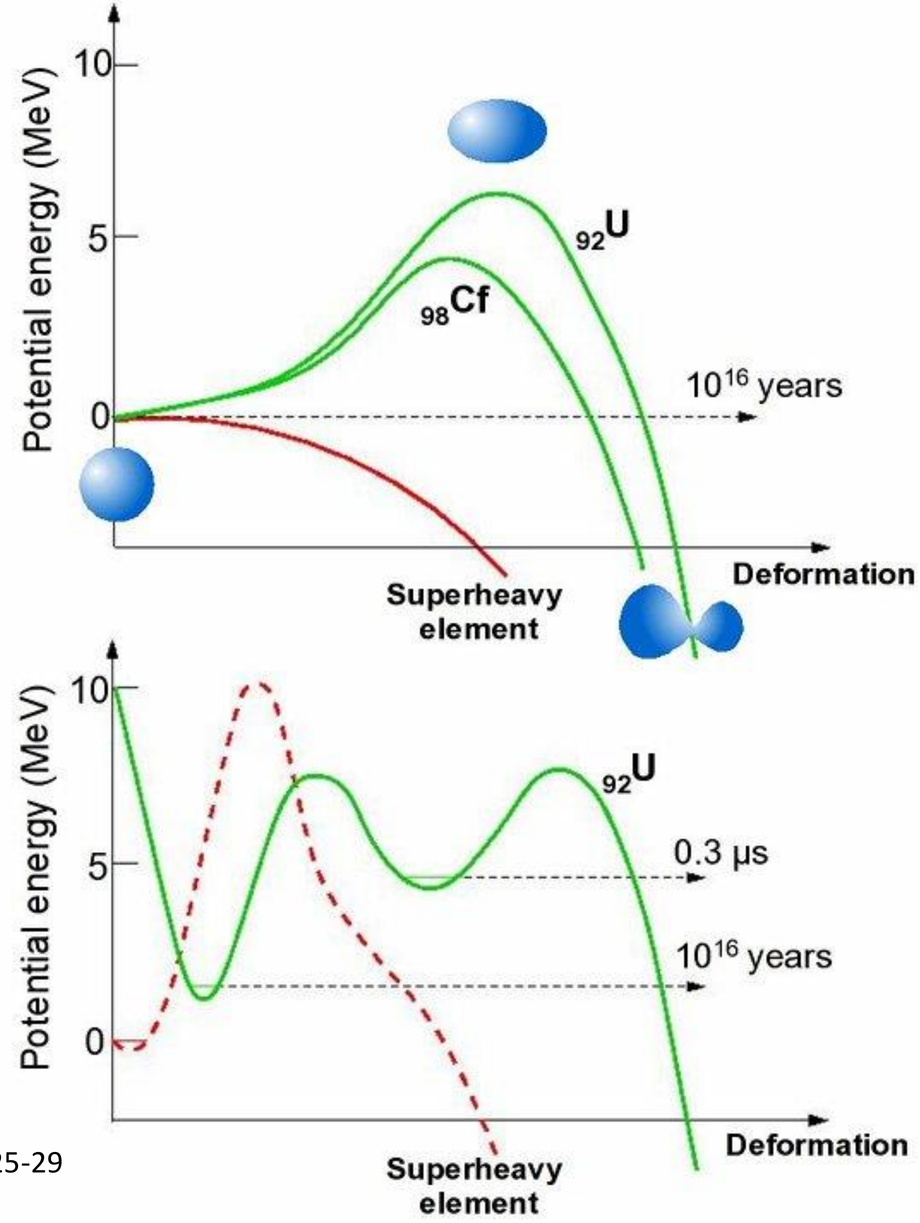

Oganessian, Yu. (2004). Superheavy elements. Physics World, 17(7), 25-29

NARODOWE CENTRUM BADAŃ JĄDROWYCH ŚWIERK

Atomic Data and Nuclear Data Tables 138 (2021) 101393

Contents lists available at ScienceDirect

Atomic Data and Nuclear Data Tables

journal homepage: www.elsevier.com/locate/adt

Properties of heaviest nuclei with $98 \leq Z \leq 126$ and $134 \leq N \leq 192$

P. Jachimowicz [a], M. Kowal [b,*], J. Skalski [b]

[a] Institute of Physics, University of Zielona Góra, Szafrana 4a, 65-516 Zielona Góra, Poland
[b] National Centre for Nuclear Research, Pasteura 7, 02-093 Warsaw, Poland

Ground-state and saddle-point shapes and masses for 1305 heavy and superheavy nuclei including odd-A and odd–odd systems. Static fission barrier heights, one- and two-nucleon separation energies, and Qα values.

Microscopic–macroscopic method with the deformed Woods–Saxon single-particle potential and the Yukawa-plus-exponential macroscopic energy taken as the smooth part.

Ground-state shapes and energies are found by the minimization over **seven axially-symmetric deformations**.
A search for saddle-points was performed by using the "imaginary water flow" method in three consecutive stages, using five- (for nonaxial shapes) and seven-dimensional (for reflection-asymmetric shapes) deformation spaces.

Good agreement with the experimental data for actinides.

Warsaw macro-micro model with rotational energy

liquid drop with a Yukawa-plus-exponential model

Strutinsky shell correction + Woods-Saxson potential + BCS

rigid body approximation

$$E_{tot}(Z,N,\beta) = E_{mac}(Z,N,\beta) + E_{mic}(Z,N,\beta) + E_{rot}(\beta,l)$$

- Allows to obtain the binding energy for a given nuclear shape β and angular momentum *l*.

Macroscopic energy E_{mac}

$$E_{mac}(Z,N,\beta) = -a_v(1-\kappa_v I^2)A + a_s(1-\kappa_s I^2)A^{2/3}B_S(\beta) + a_0A^0 + c_1Z^2A^{-1/3}B_C(\beta) - c_4Z^{4/3}A^{-1/3} - f(k_F r_p)Z^2A^{-1} + \bar{\Delta}_{mac}$$

- Liquid drop model
- Responsible for the majority of energy/mass
- Dependence on shape in the surface and Coulomb term
- Most often normalized with respect to the sphere

$$B_S = \frac{A^{-2/3}}{8\pi^2 r_0^2 a^4}\int\int_V \left(2-\frac{r_{12}}{a}\right)\frac{e^{-r_{12}/a}}{r_{12}/a}d^3r_1d^3r_2,$$

$$E_{mac}^{gs} = E_{mac}^{gs}(deformation) - E_{mac}^{gs}(sphere)$$

$$B_C = \frac{15}{32\pi^2}\frac{A^{-5/3}}{r_0^5}\int\int_V \frac{1}{r_{12}}\left[1-\left(1+\frac{1}{2}\frac{r_{12}}{a_{den}}\right)e^{-r_{12}/a_{den}}\right]d^3r_1d^3r_2$$

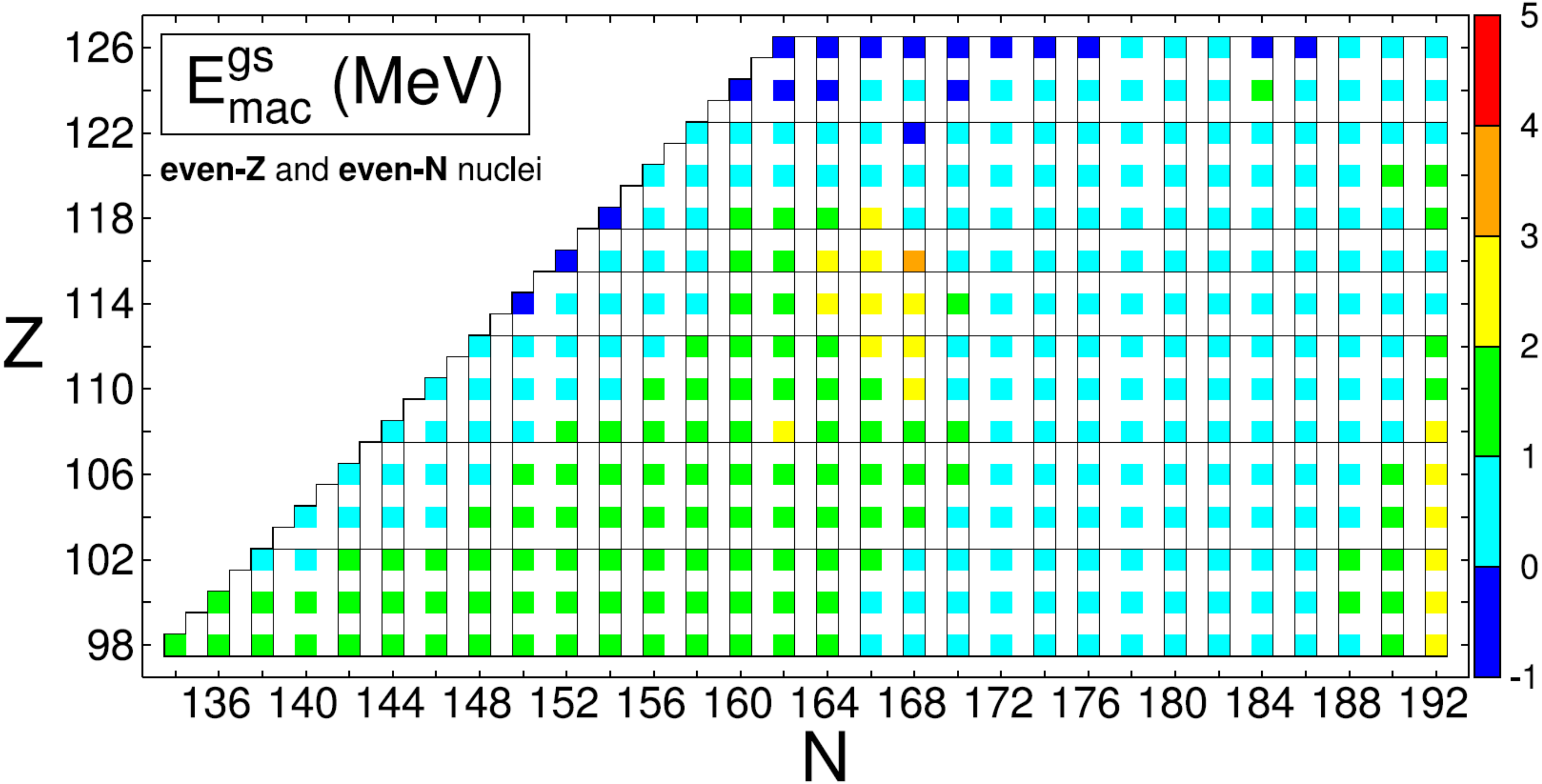

P. Jachimowicz, M. Kowal, J. Skalski, Properties of heaviest nuclei with 98≤Z≤126 and 134≤N≤192, Atomic Data and Nuclear Data Tables, Volume 138, 2021, 101393

Microscopic energy E_{mic}

$$E_{mic}(Z,N,\beta) = E^{sh}_{corr}(Z,N,\beta) + E^{pair}_{corr}(Z,N,\beta)$$

- Strutinsky shell correction based on the deformed Woods–Saxon single-particle potential

$$V_{WS}(\vec{r}) = -\frac{V}{1+e^{d(\vec{r},\beta)/a_{ws}}}$$

- The single-particle potential is diagonalized in the deformed harmonic-oscillator basis
- Pairing energy, pair correlation from Bardeen–Cooper–Schrieffer (BCS) theory

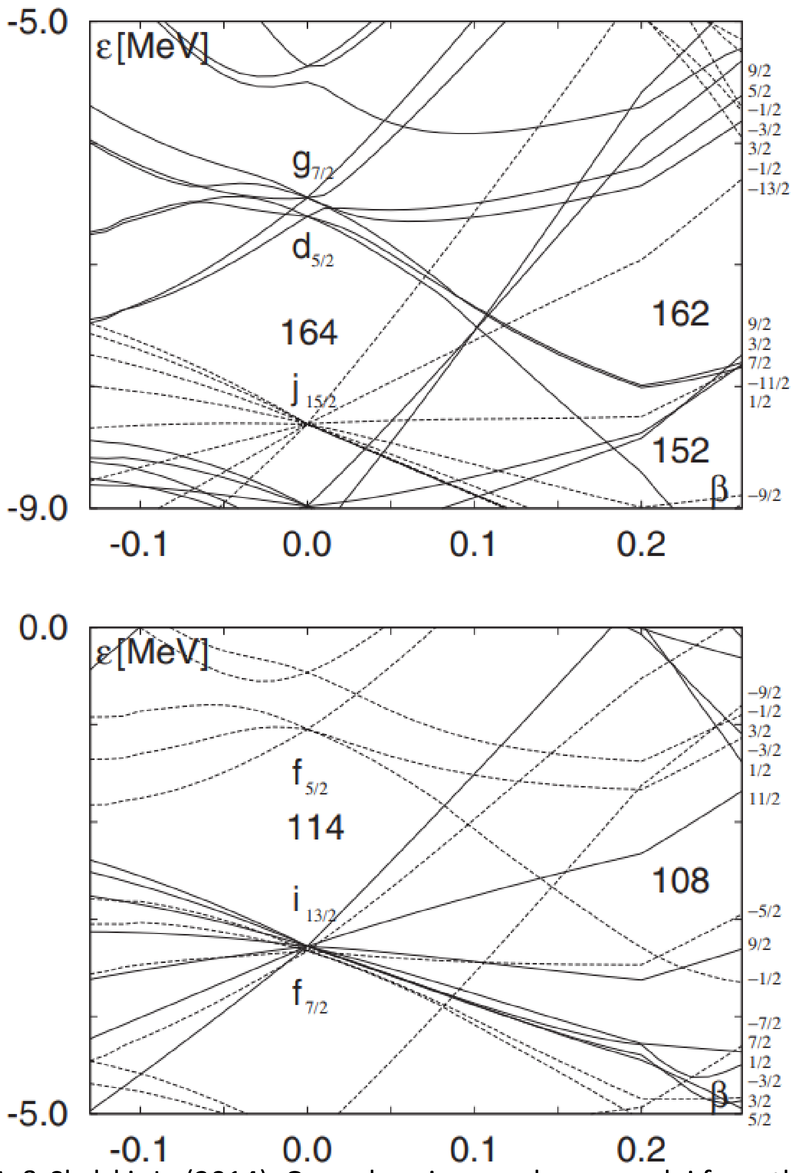

Jachimowicz, P. & Kowal, M. & Skalski, J.. (2014). Q α values in superheavy nuclei from the deformed Woods-Saxon model. Physical Review C. 89. 10.1103/PhysRevC.89.024304.

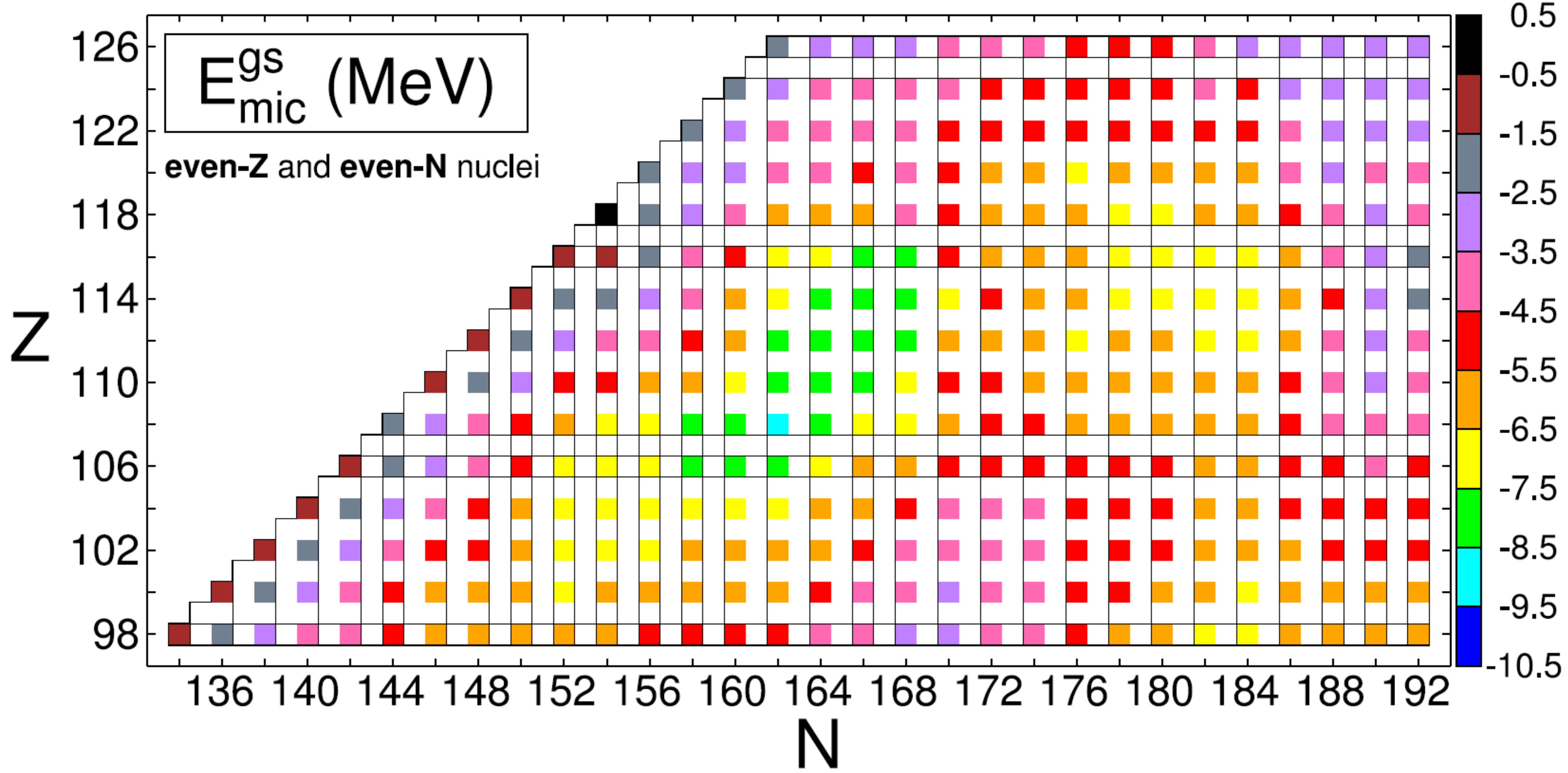

P. Jachimowicz, M. Kowal, J. Skalski, Properties of heaviest nuclei with 98≤Z≤126 and 134≤N≤192, Atomic Data and Nuclear Data Tables, Volume 138, 2021, 101393

NARODOWE CENTRUM BADAŃ JĄDROWYCH ŚWIERK

Rotational energy E_{rot}

- Rigid body approximation
- Moment of inertia calculated analytically

$$E_{rot} = l(l+1)\frac{(\hbar c)^2}{2I(\beta)} \qquad \mathbf{I} = \begin{pmatrix} I_\perp & & \\ & I_\perp & \\ & & I_\parallel \end{pmatrix}$$

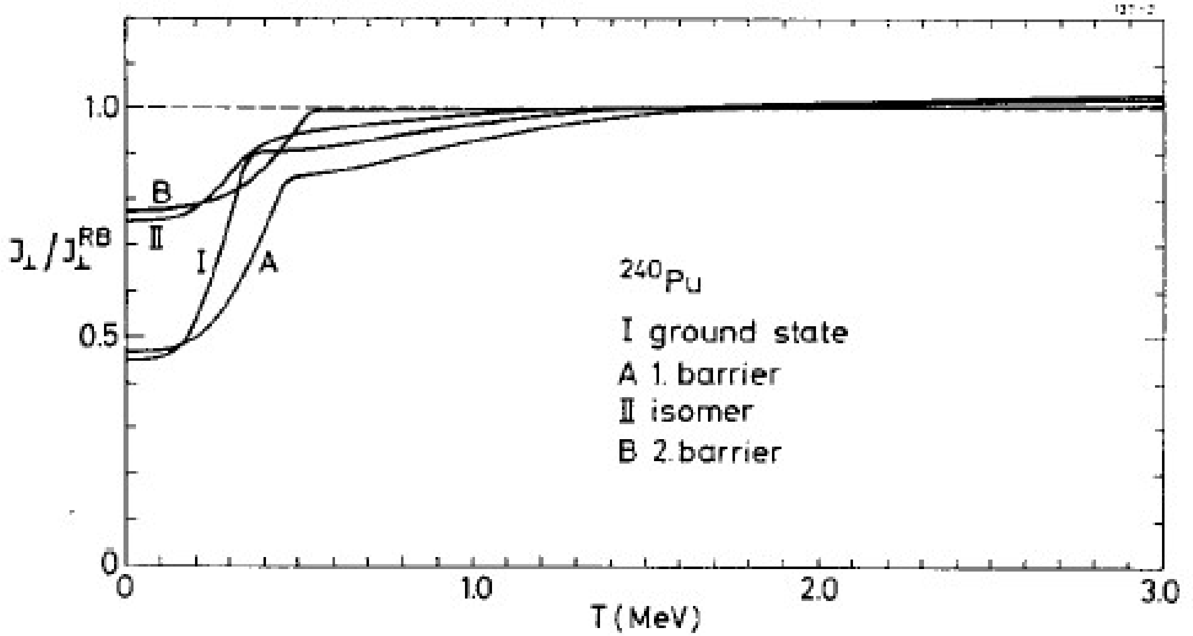

M. Brack, T. Ledergerber, H. Pauli, A. Jensen, Nuclear Physics A **234**, 185–215 (1974)

$$I_\perp = \frac{1}{5}\rho R_0{}^5 \int \sin(\theta)(\pi\sin^2(\theta) + 2\pi\cos^2(\theta))(1 + \frac{1}{2}\sqrt{\frac{3}{\pi}}\beta_{10}\cos(\theta) + \frac{1}{4}\sqrt{\frac{5}{\pi}}\beta_{20}(3\cos^2(\theta) - 1)$$
$$+ \frac{1}{4}\sqrt{\frac{7}{\pi}}\beta_{30}(5\cos^3(\theta) - 3\cos(\theta)) + \frac{1}{16}\sqrt{\frac{9}{\pi}}\beta_{40}(35\cos^4(\theta) - 30\cos^2(\theta) + 3))^5 d\theta$$

NARODOWE CENTRUM BADAŃ JĄDROWYCH ŚWIERK

Shape parametrization

- An expansion of the nuclear radius R(θ, ϕ) onto spherical harmonics $Y_{\lambda\mu}(\theta, \phi)$ is used:

$$R(\vartheta, \varphi) = cR_0\{1 + \sum_{\lambda=1}^{\infty} \beta_{\lambda 0} Y_{\lambda 0}(\vartheta, \varphi)\}$$

- For now, shapes in random walk method are limited to axially symmetrical ($\mu = 0$) and depend only on $\underline{\beta_{10}}$, β_{20}, β_{30} and β_{40}.

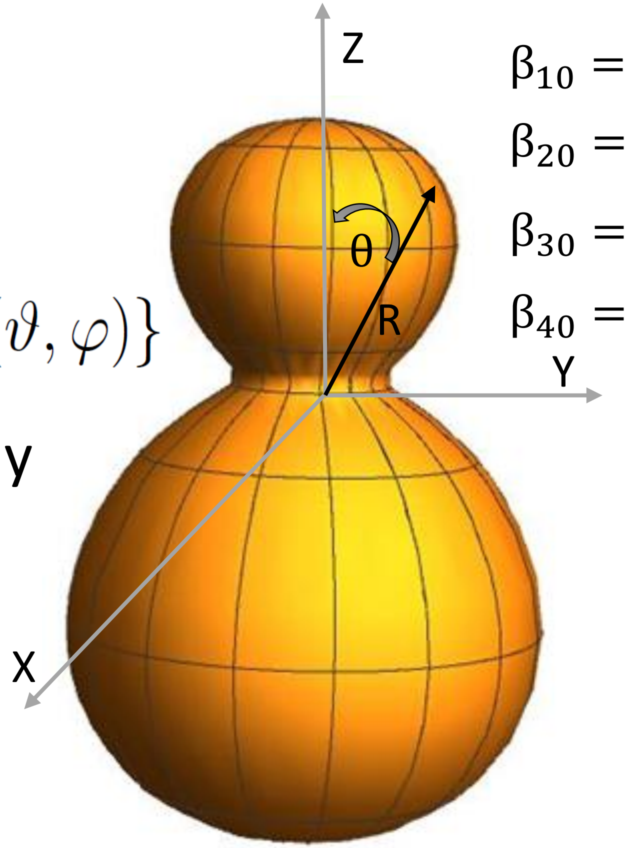

$\beta_{10} = +0.93$
$\beta_{20} = +1.65$
$\beta_{30} = +0.00$
$\beta_{40} = -0.25$

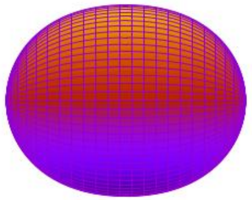

Compound nucleus

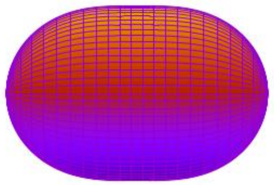

Fission saddle point

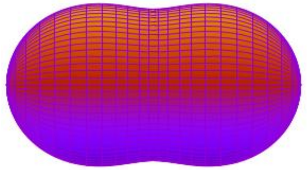

2nd minimum

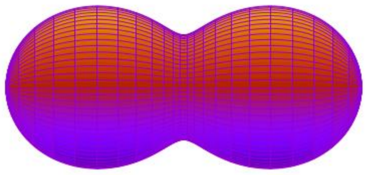

Scission point symmetrical fission

Shape parametrization

- β_{10} – dipole
- β_{20} – quadrupole/elongation
- β_{30} – hexadecople/asymmetry
- β_{40} – octupole/neck parameter
- β_{10} used as an actual shape parameter

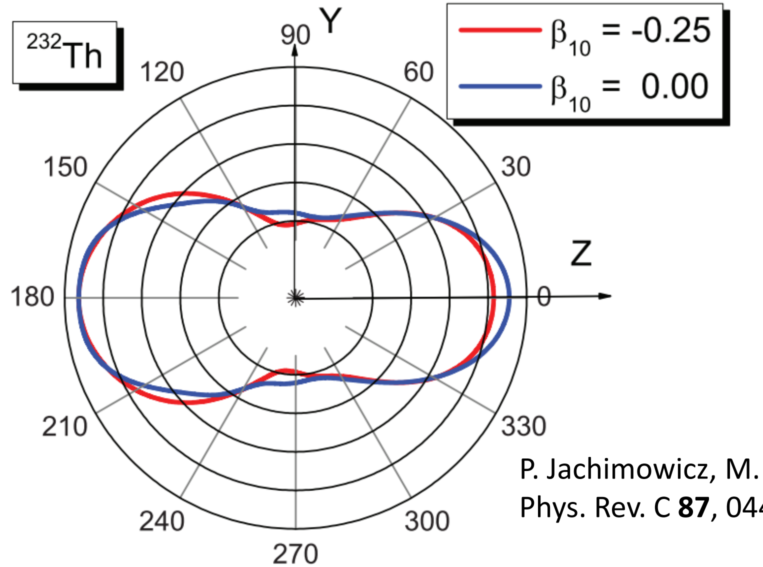

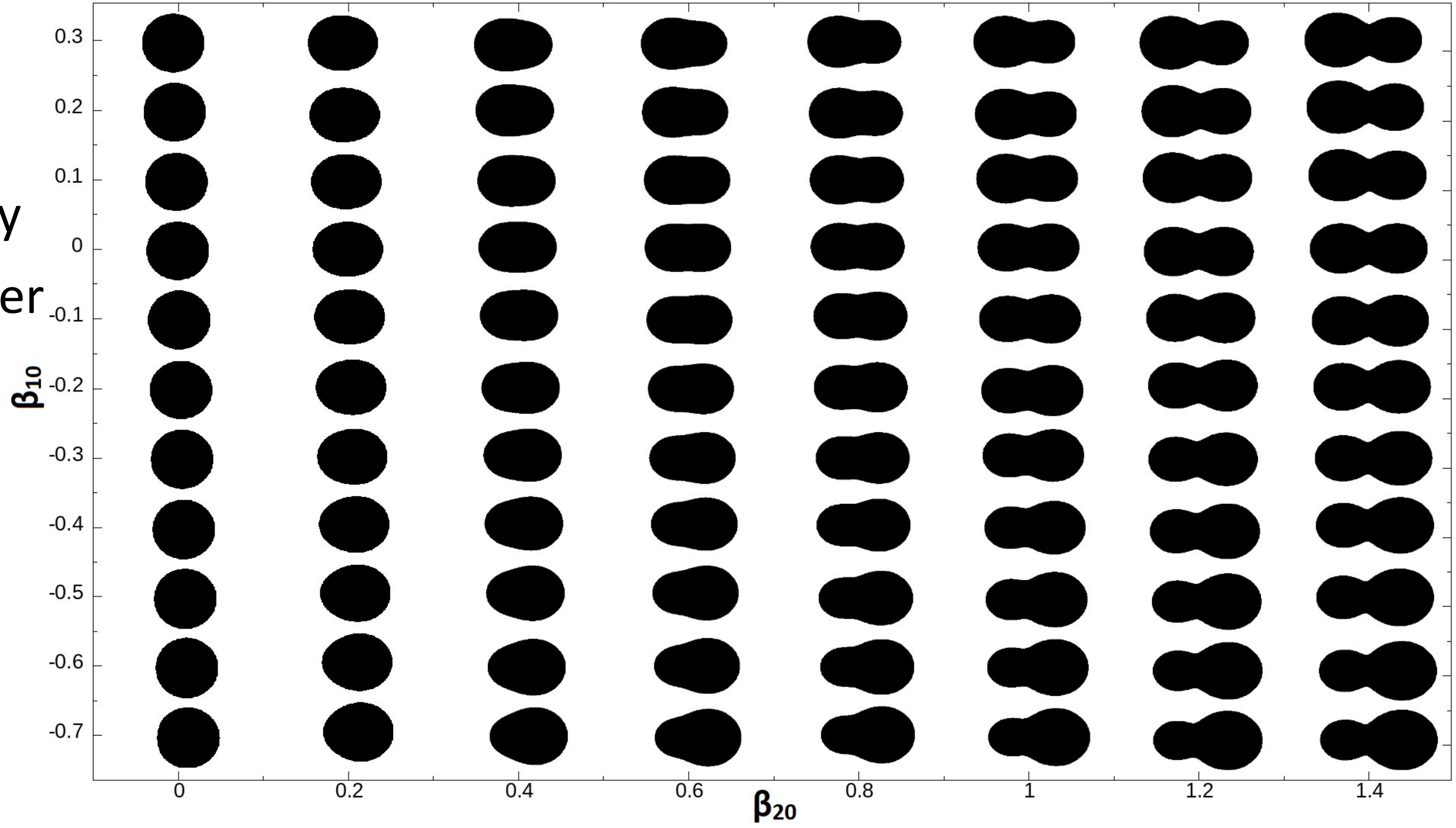

P. Jachimowicz, M. Kowal, and J. Skalski, Phys. Rev. C **87**, 044308 (**2013**)

Shape parametrization

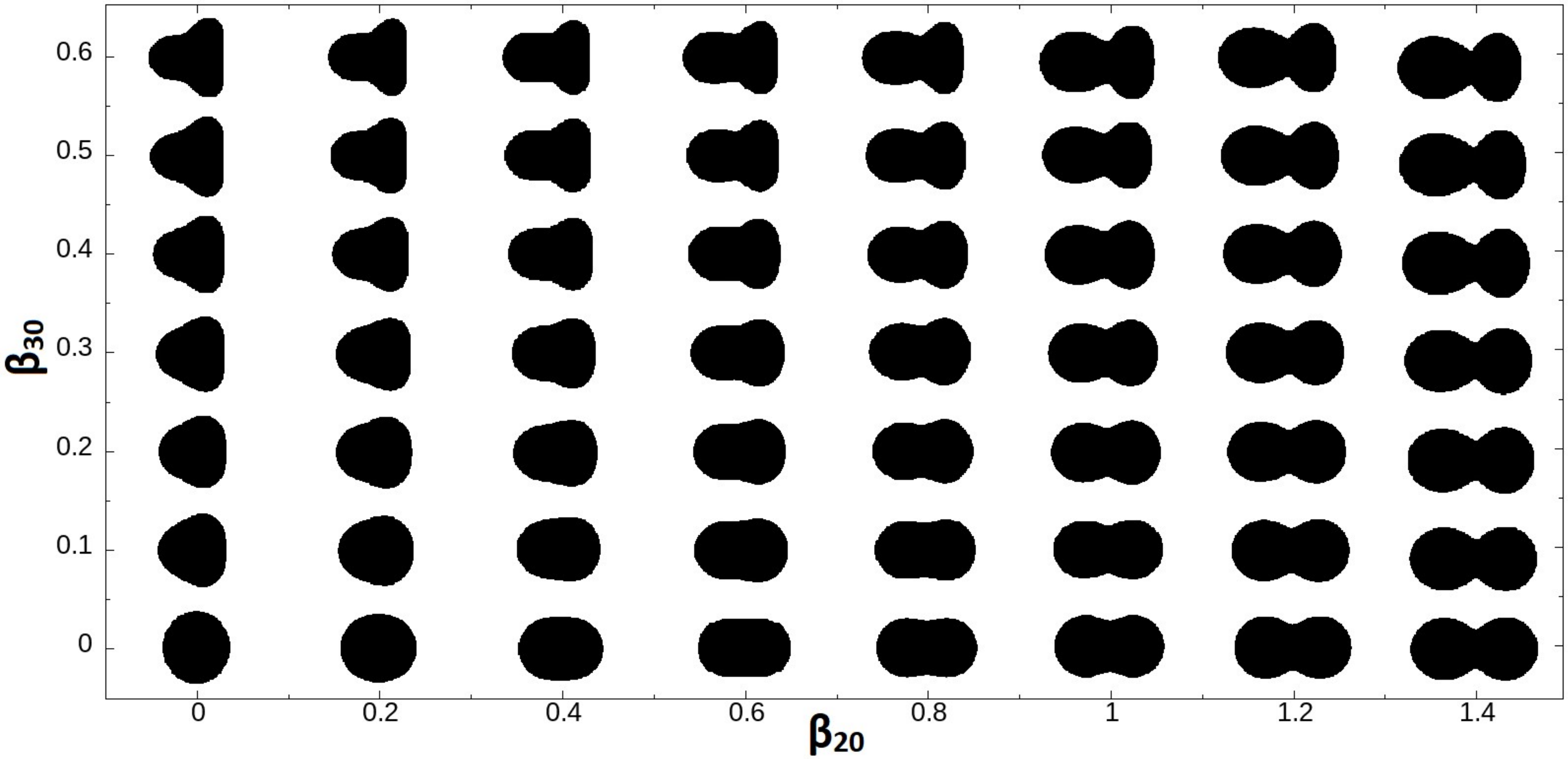

NARODOWE CENTRUM BADAŃ JĄDROWYCH ŚWIERK

Shape parametrization

- β_{40} is crucial in the beginning of the fusion process and during scission

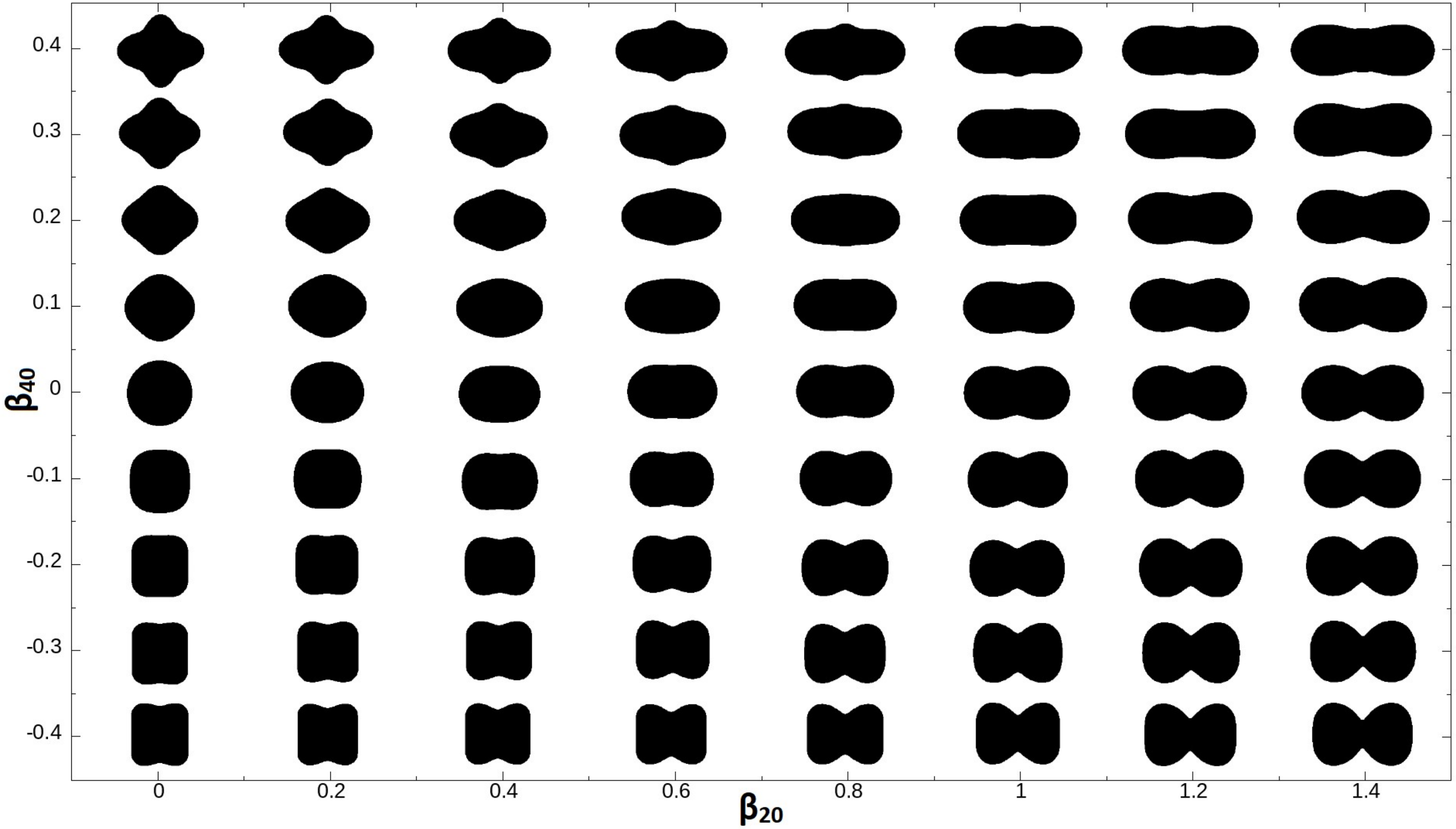

Starting point parametrization

- After overcoming the entrance channel barrier, the projectile and the target are assumed to be in a touching configuration.
- The spherical harmonic parametrization is fitted, with the origin situated in the neck, giving the β parameters for the starting point configuration.
- The shapes are asymmetrical, but β_{30} is near to 0, thanks to the inclusion of β_{10}.
- Calculations were done for ^{54}Cr spherical and deformed (least optimal for fusion).

System	β_{10}	β_{20}	β_{30}	β_{40}
^{48}Ca+^{208}Pb	0.93	1.65	0.0	-0.24
^{50}Ti+^{208}Pb	0.92	1.75	0.01	-0.30
^{54}Cr(spherical)+^{208}Pb	-0.87	1.75	-0.01	-0.30
^{54}Cr(deformed)+^{208}Pb	-0.94	1.83	0.18	-0.16

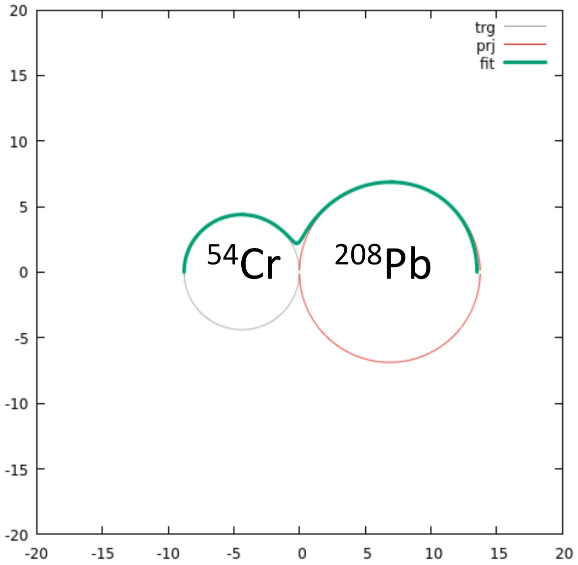

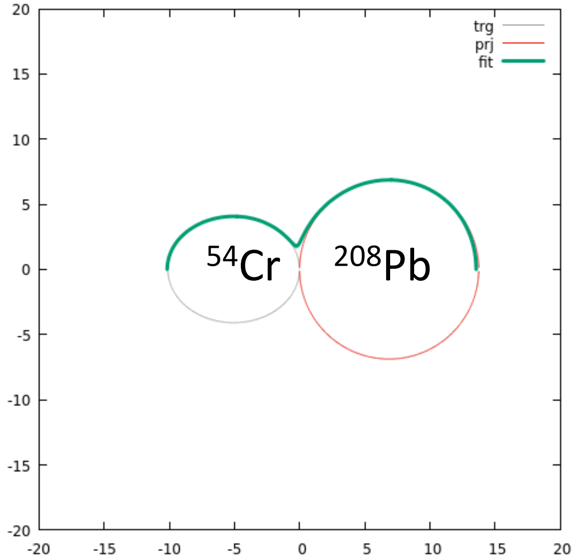

Potential energy surfaces

asymmetry

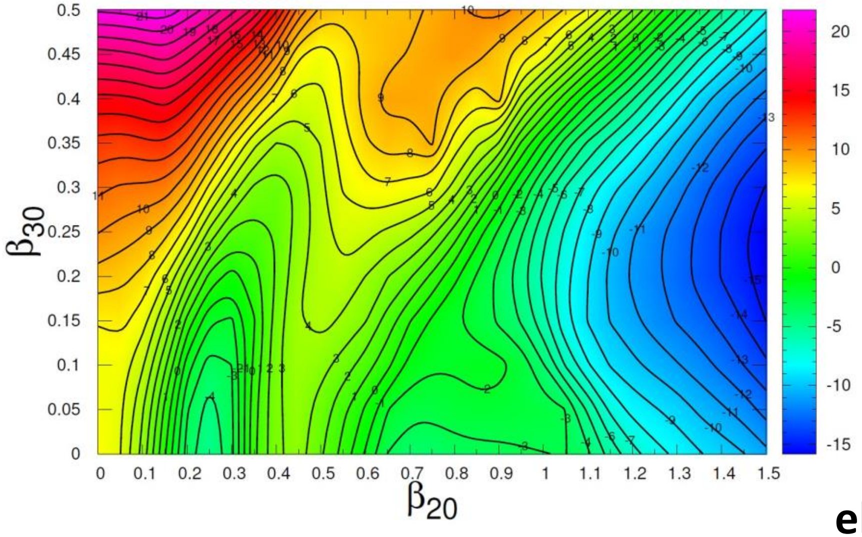

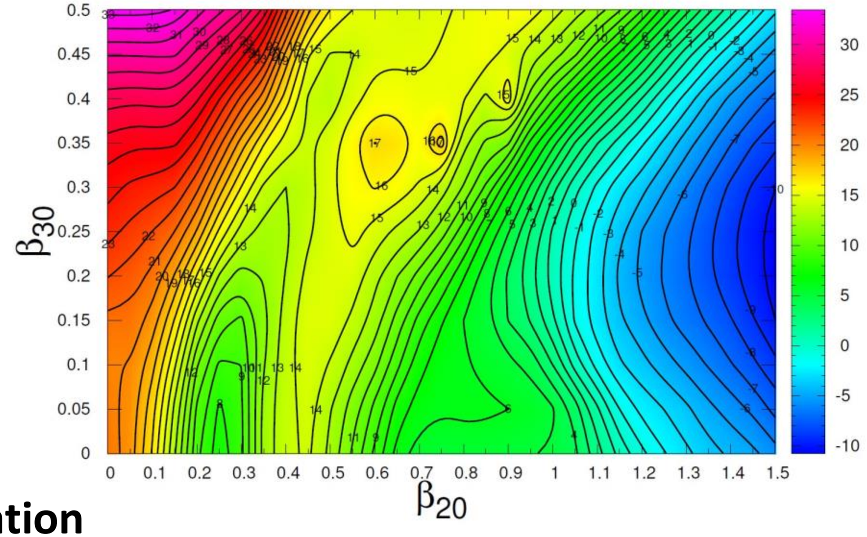

$^{48}Ca + {}^{208}Pb$

$l = 0$

elongation

$^{48}Ca + {}^{208}Pb$

$l = 60$

neck parameter

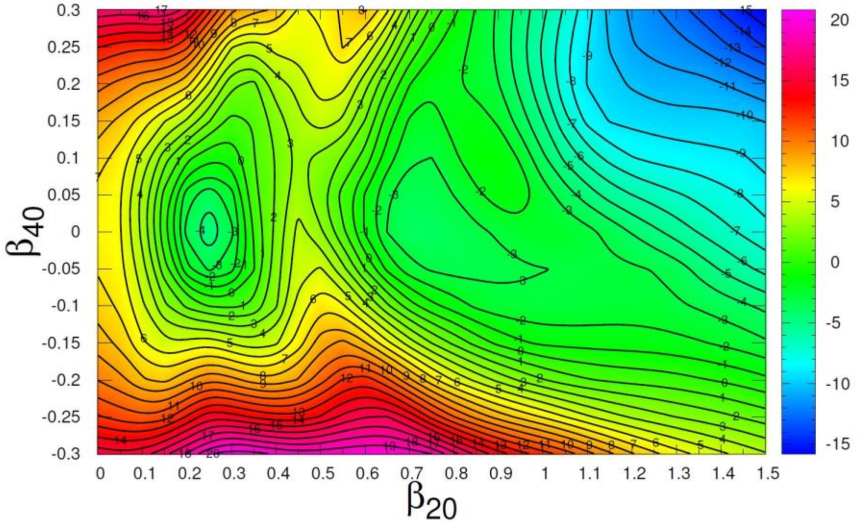

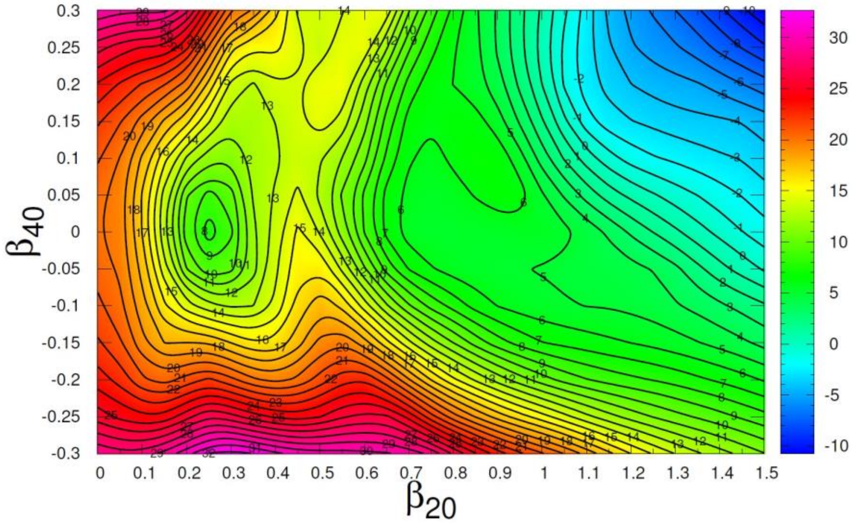

Potential energy surfaces

asymmetry

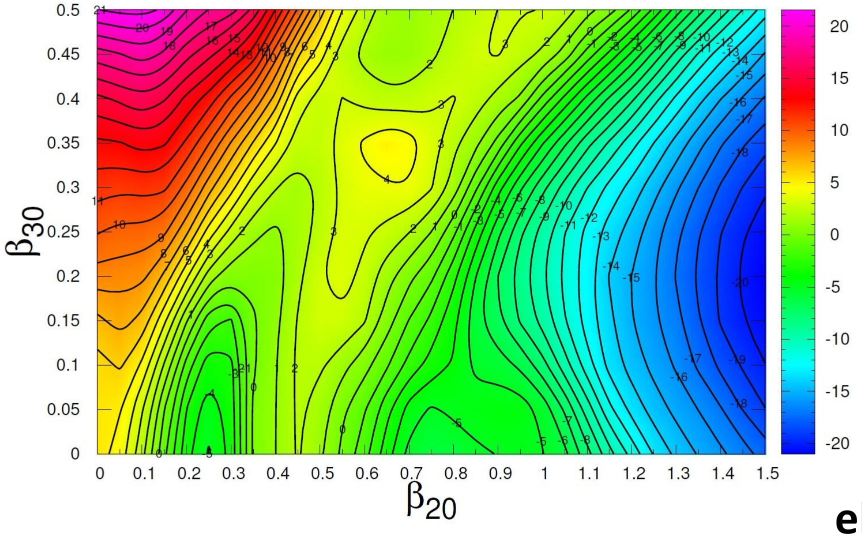

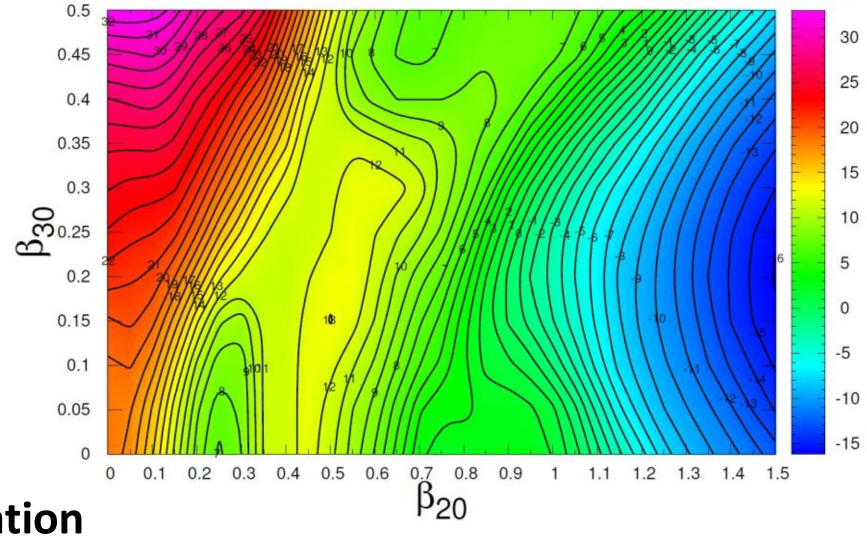

^{54}Cr+ ^{208}Pb
l = 0

elongation

^{54}Cr+ ^{208}Pb
l = 60

neck parameter

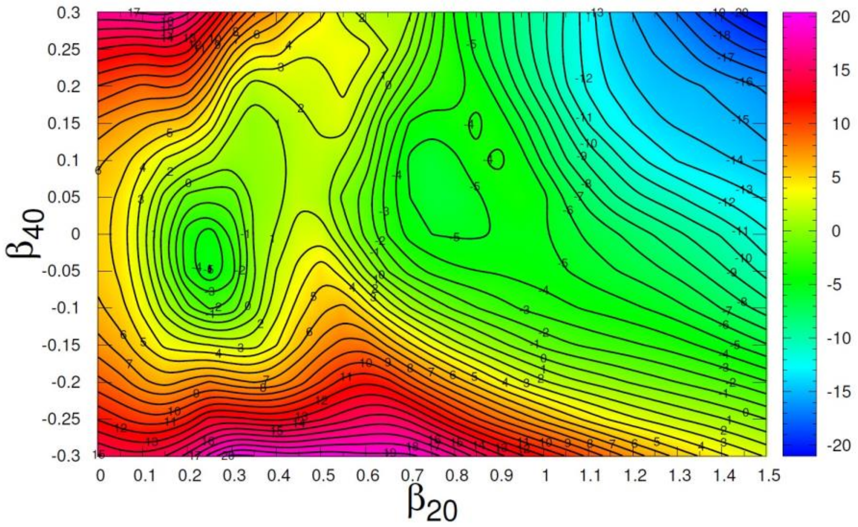

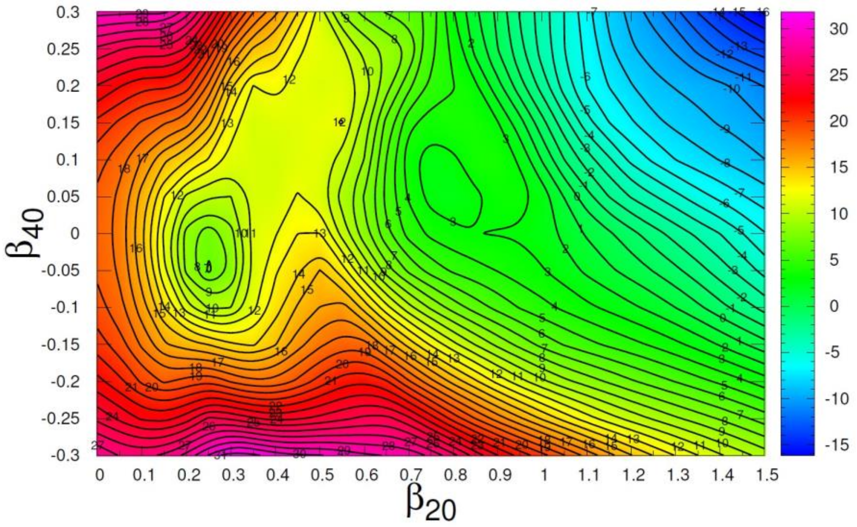

Random walk method

- The probability of transitioning from one shape to another is determined by the number of available energy levels for a given shape β.

$$N_i(\beta_i) \propto \exp\left(2\sqrt{a(E^*(\beta_i) - E_{rot}(\beta_i))}\right)$$

a – constant density parameter

- Only one β parameter changes at a time, by a step of 0.05, giving 8 possible directions of movement.

^{48}Ca+ ^{208}Pb

$l = 0$

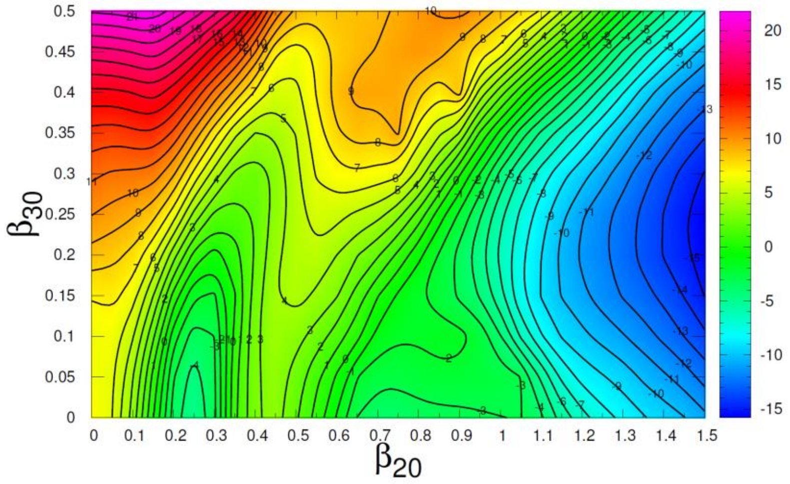

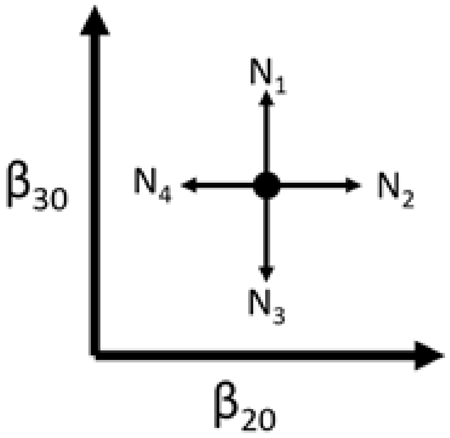

$$P_i = \frac{N_i(\beta_i)}{\Sigma_j N_j(\beta_j)}$$

- Fusion: $\beta_{20} <= 0.3$, $\beta_{30} <= 0.2$, $\beta_{40} <= 0.2$ → compound nucleus.
- Fission: when the thickness of the neck connecting the fission fragments is less than 4.0 fm.

Example of a paths

$^{54}Cr + ^{208}Pb$

$E^* = 50$ MeV, $l = 40$

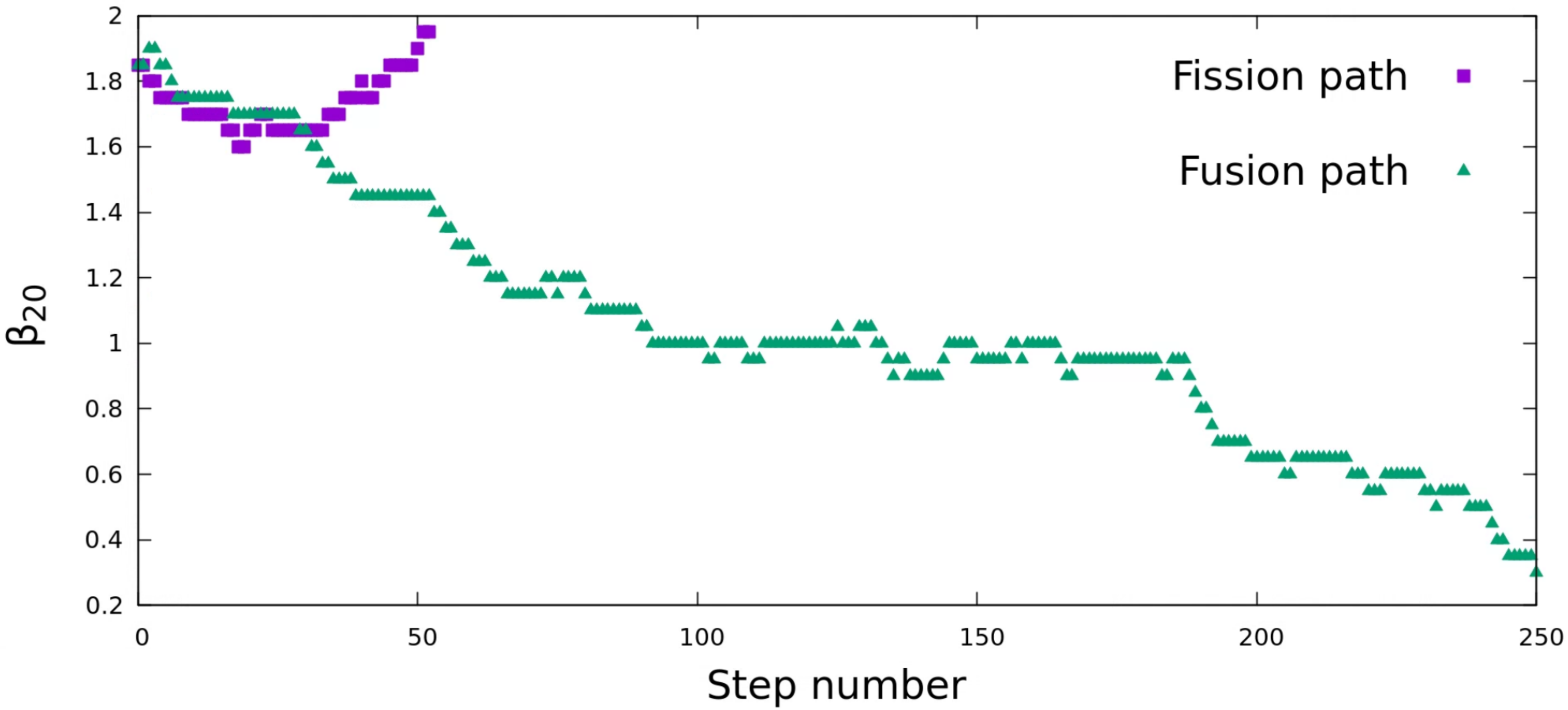

Example of a paths

$^{54}Cr + {}^{208}Pb$

$E^* = 50$ MeV, $l = 40$

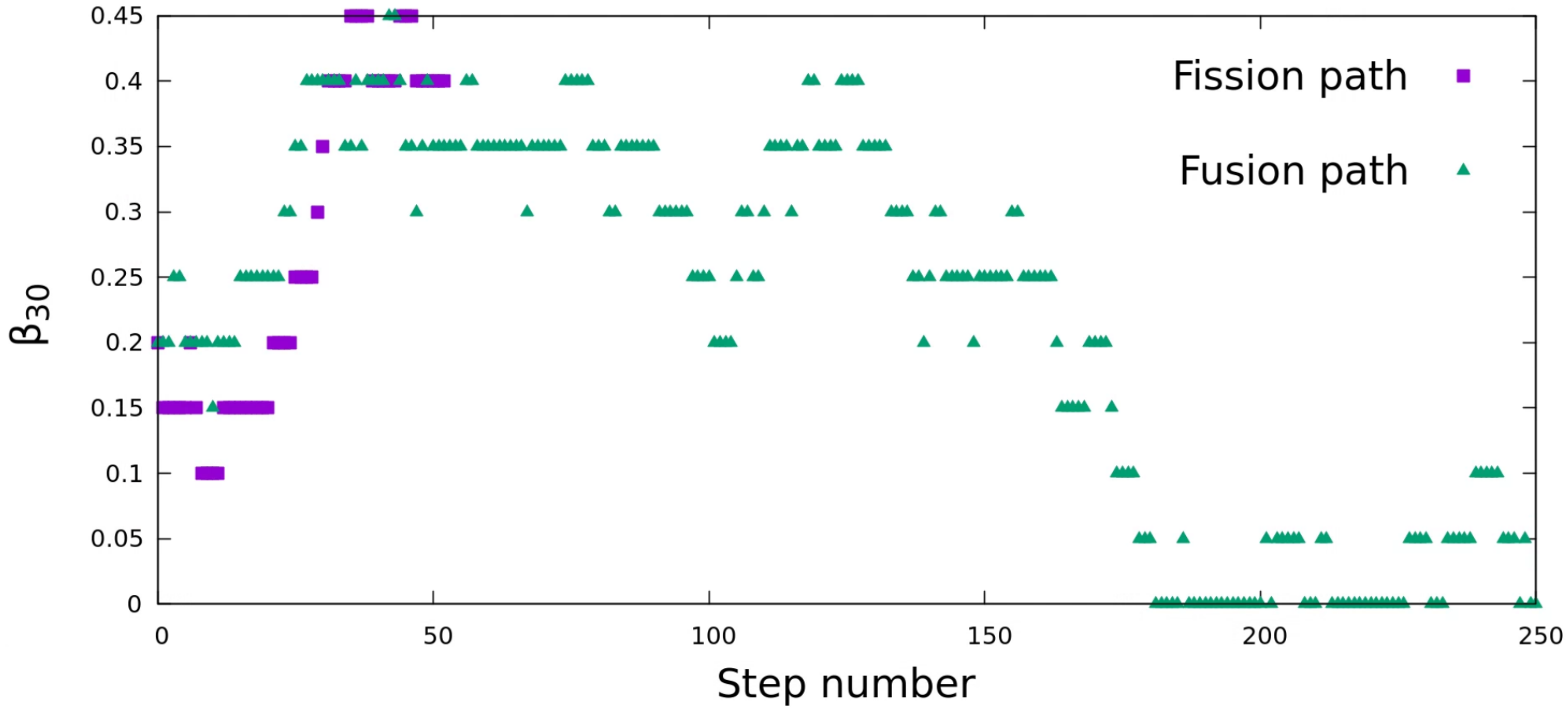

NARODOWE CENTRUM BADAŃ JĄDROWYCH ŚWIERK

Example of a paths

$^{54}Cr + ^{208}Pb$

$E^* = 50$ MeV, $l = 40$

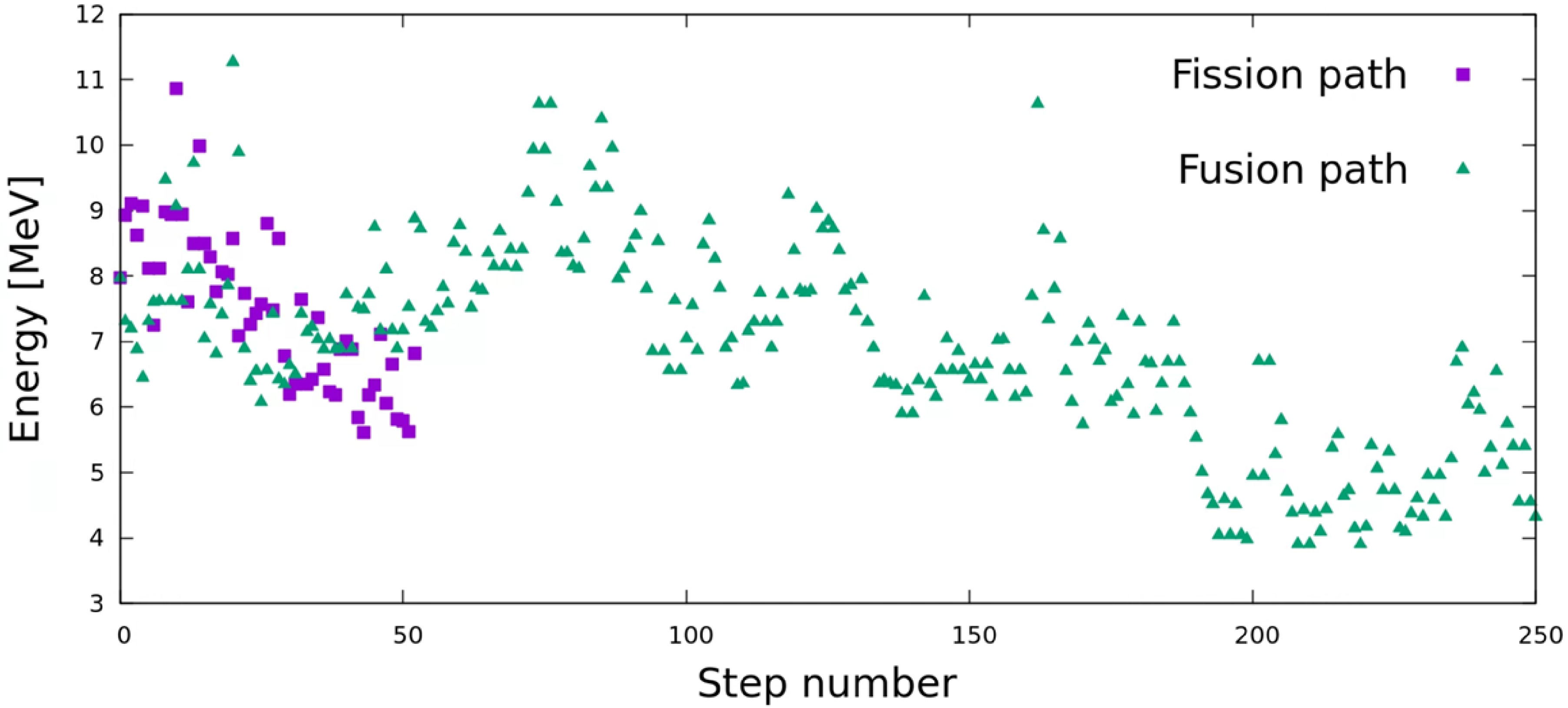

Random walk method

- Calculations were done for excitation energies from 20 to 70 MeV with 1 MeV step. 10000 paths were calculated for a given energy and *l*-value from 0 to l_{max}. $P_{fus}(E_{cm}, l)$ is given as a ratio of the number of paths that lead to fusion to the total number of paths

$$P_{fus}(E_{cm}, l) = \frac{\text{paths which ended in fusion}}{10000}$$

- ~ 3600 E^* and *l* combinations → ~36 million paths per reaction
- Average over *l* to get P_{fus} dependant on E_{cm}:

$$P_{fus}(E_{cm}) = \frac{\sum_{l=0}^{lmax}(2l+1)P_{fus}(l)}{(2l_{max}+1)^2}$$ fusion probability averaged over l

Capture and fusion cross section

- Capture cross section calculated from FbD model
- Fusion cross section from the random walk method $\sigma_{fus} = \pi \lambda\!\!\!^{-2} \sum_{l=0}^{l_{max}} (2l+1) T(l) P_{fus}(l) = \sigma_{cap} \times P_{fus}$
- Distributions of $\frac{d\sigma_{cap}}{dl}$ (black) and $\frac{d\sigma_{fus}}{dl}$ (red) for ^{48}Ca+ ^{208}Pb

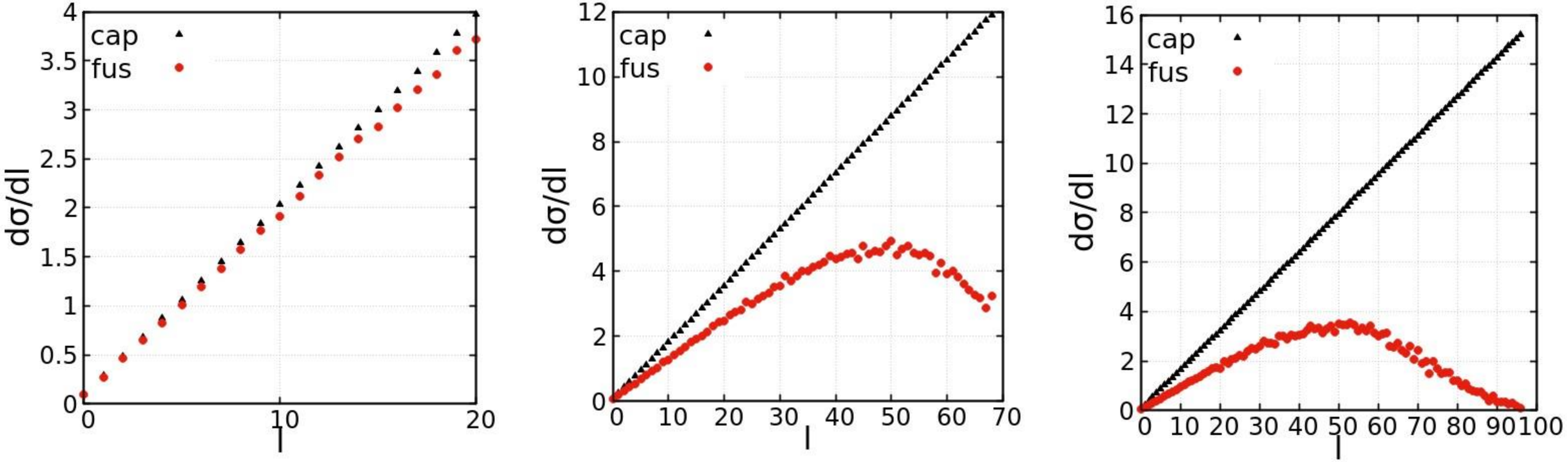

E* = 20 MeV E* = 40 MeV E* = 60 MeV

Fusion probability from the random walk

$$P_{fus}(E_{cm}) = \frac{\sum_{l=0}^{lmax}(2l+1)P_{fus}(l)}{(2l_{max}+1)^2}$$ fusion probability averaged over l

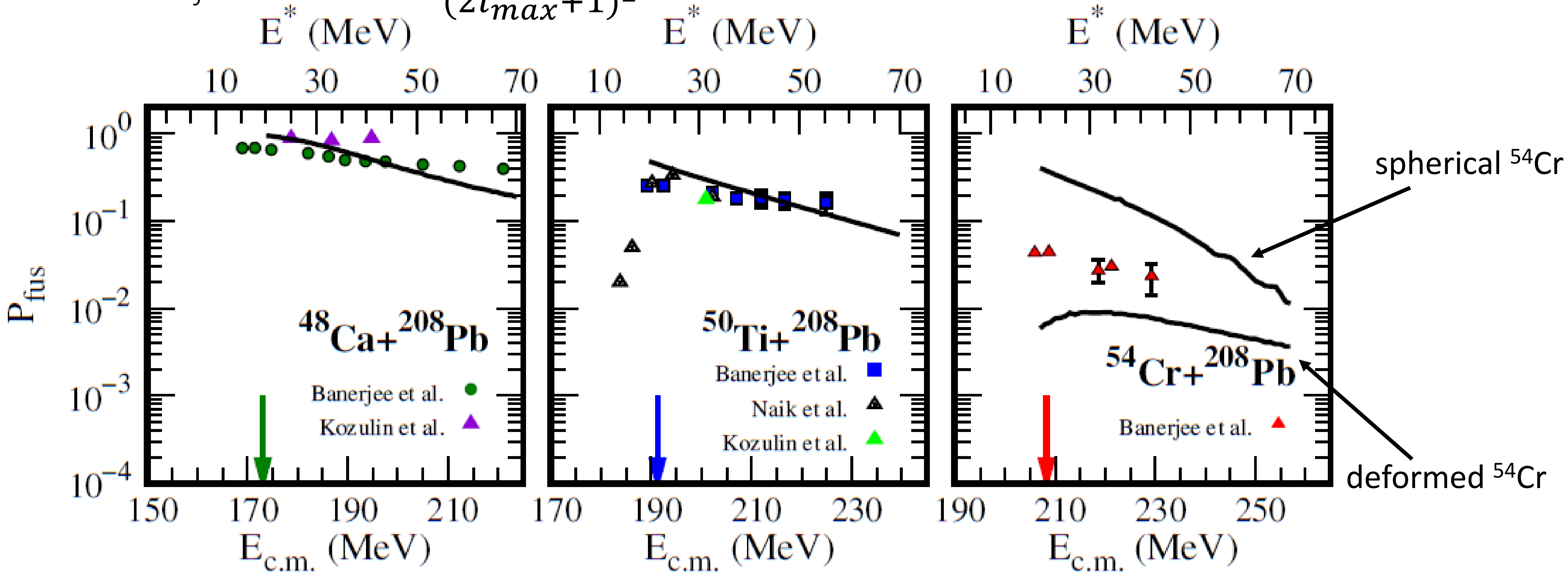

The averaged fusion probability, shown as solid, black lines, calculated with the random walk method, for the reactions 48Ca+208Pb, 50Ti+208Pb and 54Cr+208Pb. For comparison, experimental results obtained in [K. Banerjee et al., PRL 122, 232503 (2019)] and [E. M. Kozulin et al., NPA 802, 45 (2008)] are also shown. The arrows indicate the value of the mean entrance channel barrier for each reaction

NARODOWE CENTRUM BADAŃ JĄDROWYCH ŚWIERK

Fusion probability from FbD model

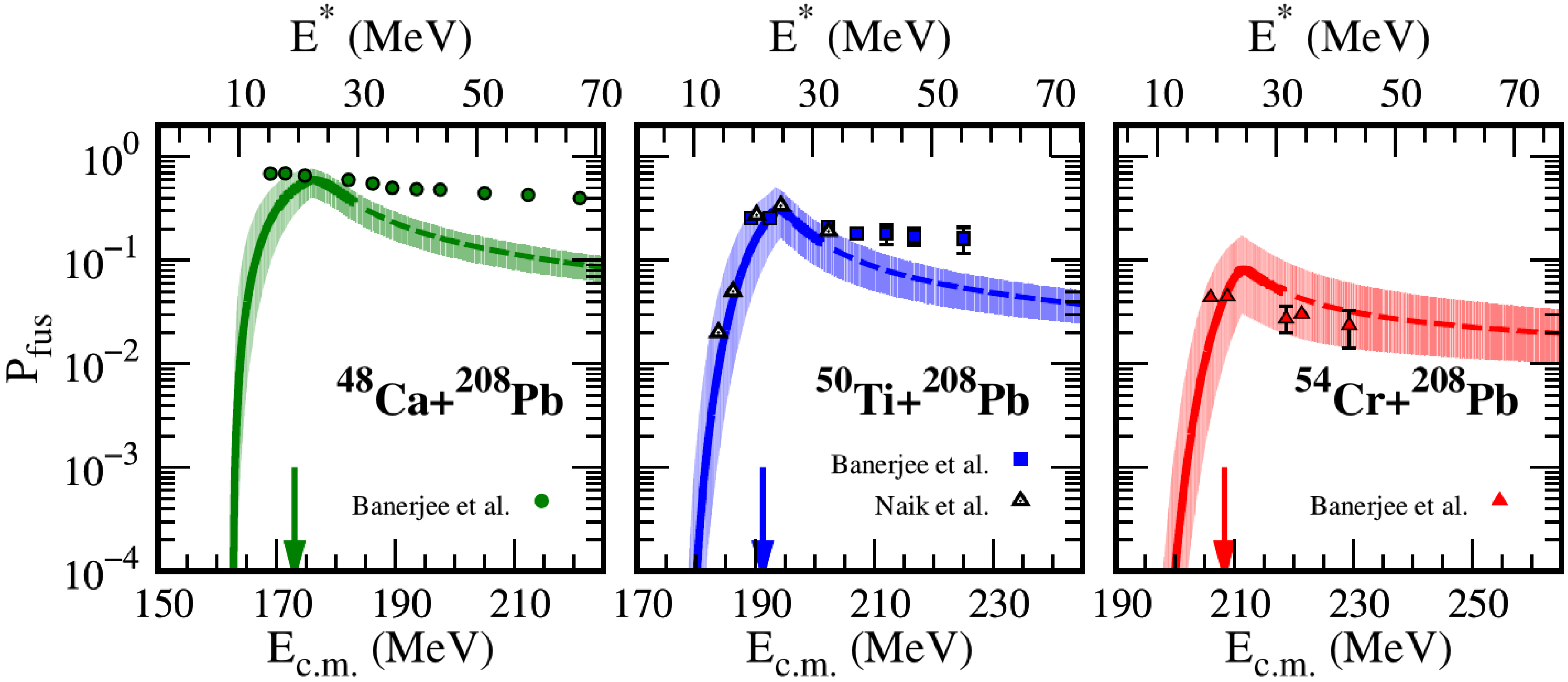

T. Cap, M. Kowal, and K. Siwek-Wilczyńska, Phys. Rev. C **105**, L051601 (2022)

NARODOWE CENTRUM BADAŃ JĄDROWYCH ŚWIERK

Mass distribution of fission fragments

- The final fission shapes can be divided, and their volumes compared, giving the mass distribution of fission fragments, for each E^* and *l*.

$^{54}Cr + ^{208}Pb$

$E^* = 30$ MeV, $l = 20$

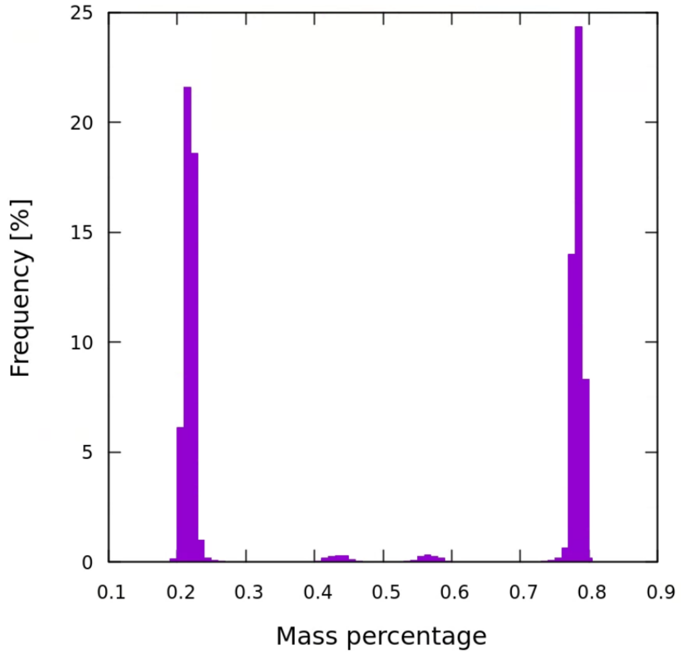

$^{54}Cr + ^{208}Pb$

$E^* = 50$ MeV, $l = 40$

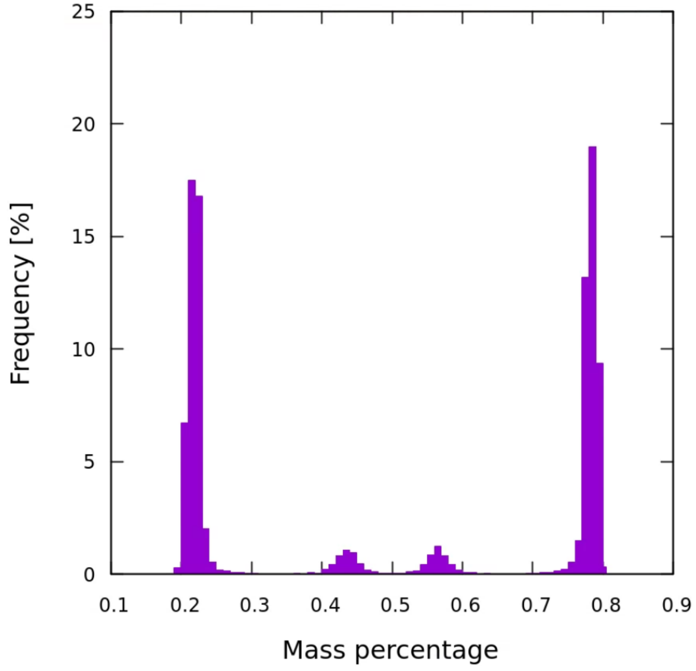

$^{54}Cr + ^{208}Pb$

$E^* = 70$ MeV, $l = 70$

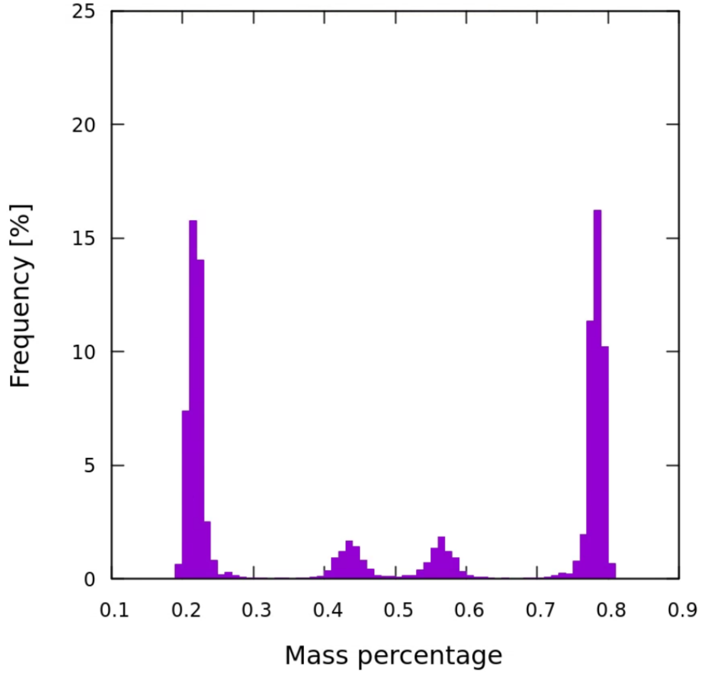

NARODOWE CENTRUM BADAŃ JĄDROWYCH ŚWIERK

Summary

- The random walk method reproduces experimental results for spherical pairs of targets and projectiles. For deformed systems, limited to only axially symmetric shapes, the model gives a lower limit of P_{fus} which is an order of magnitude smaller than the data. To properly describe such systems, the method would have to be expanded to non-axially symmetric shapes and would have to incorporate multiple possible starting points depending on the orientation of the target and the projectile.
- The random walk method looks to be a promising direction of study to better understand the fusion probability in reactions leading to the synthesis of superheavy nuclei.

Next steps

- Expand to 8 $\beta_{\lambda 0}$ dimensions
- Determine optimal step size for each β parameter
- Expand to non-axially symmetric shapes ($\beta_{\lambda\mu}$) and incorporate multiple possible starting points depending on the orientation of the target and the projectile
- Introduce a density parameter beyond Fermi gas model
- Incorporate shell-correction damping
- Allow for the emission of neutrons, protons and alfa particles during the random walk
- Calculate P_{fus} for other cold fusion reactions
- Calculate P_{fus} for hot fusion reactions, both already performed and planned experiments

Emission of neutrons, protons and alfa particles during the random walk

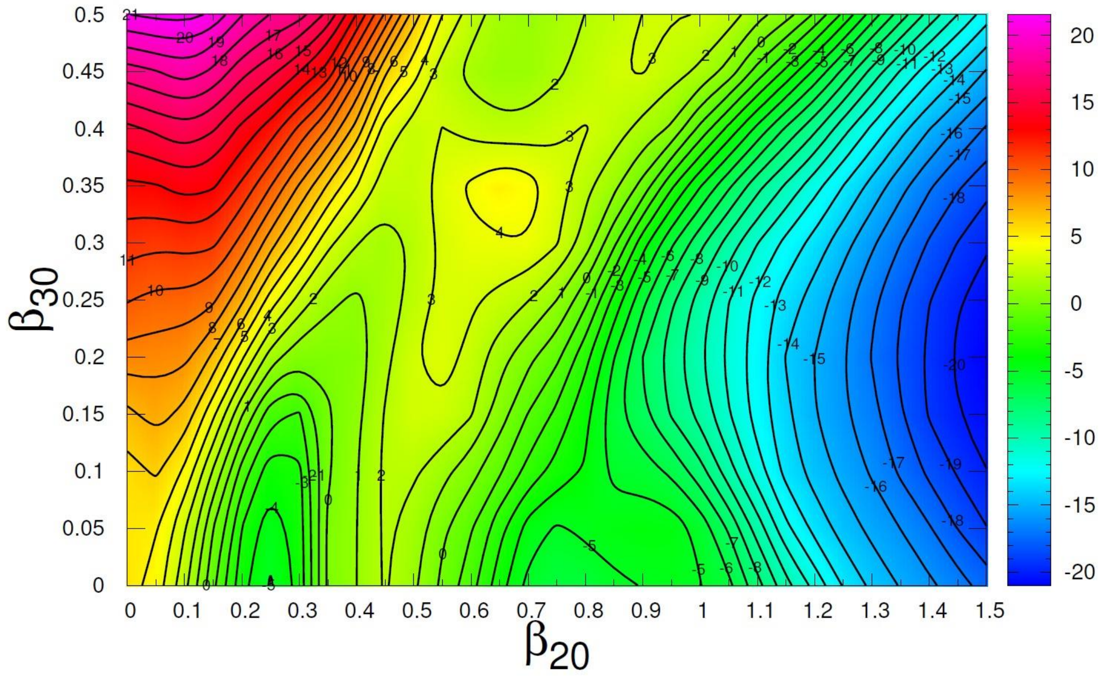

$^{54}Cr + ^{208}Pb$, $I = 0$

-2 neutrons

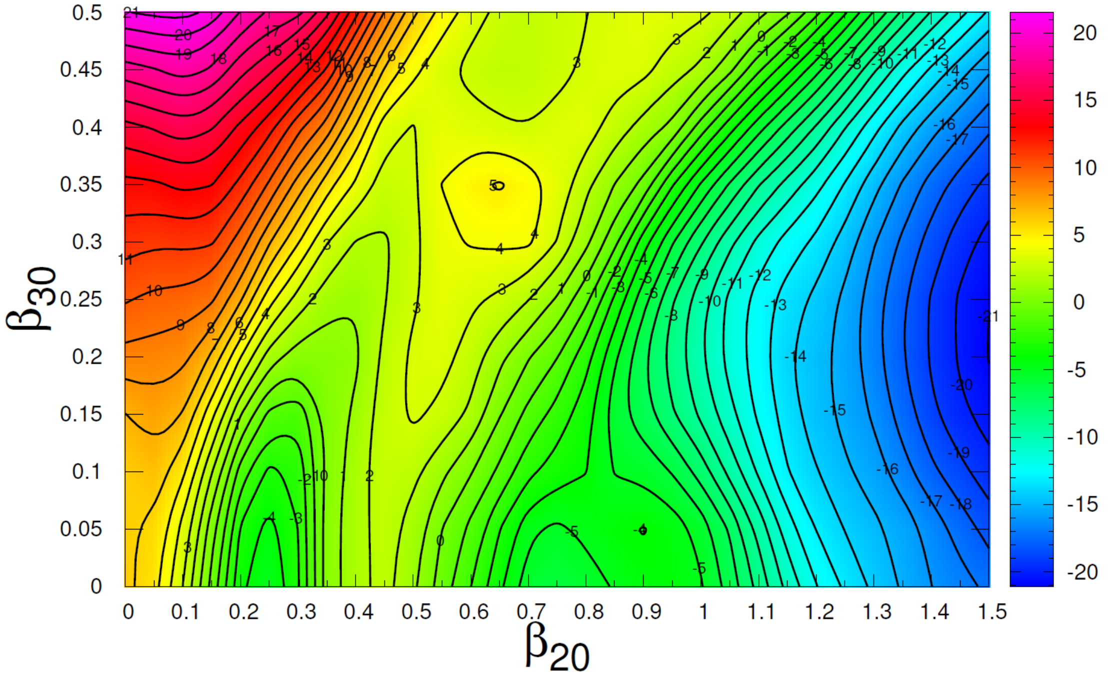

$^{52}Cr + ^{208}Pb$, $I = 0$

Instead of moving only between shapes, we can also change the PESs.

Thank you for your attention !

NATIONAL
CENTRE
FOR NUCLEAR
RESEARCH
ŚWIERK

www.ncbj.gov.pl

BONUS SLIDES

In the **FBD** model, we use 1D motion approximation

The system must overcome an internal barrier ***H*** to fuse.

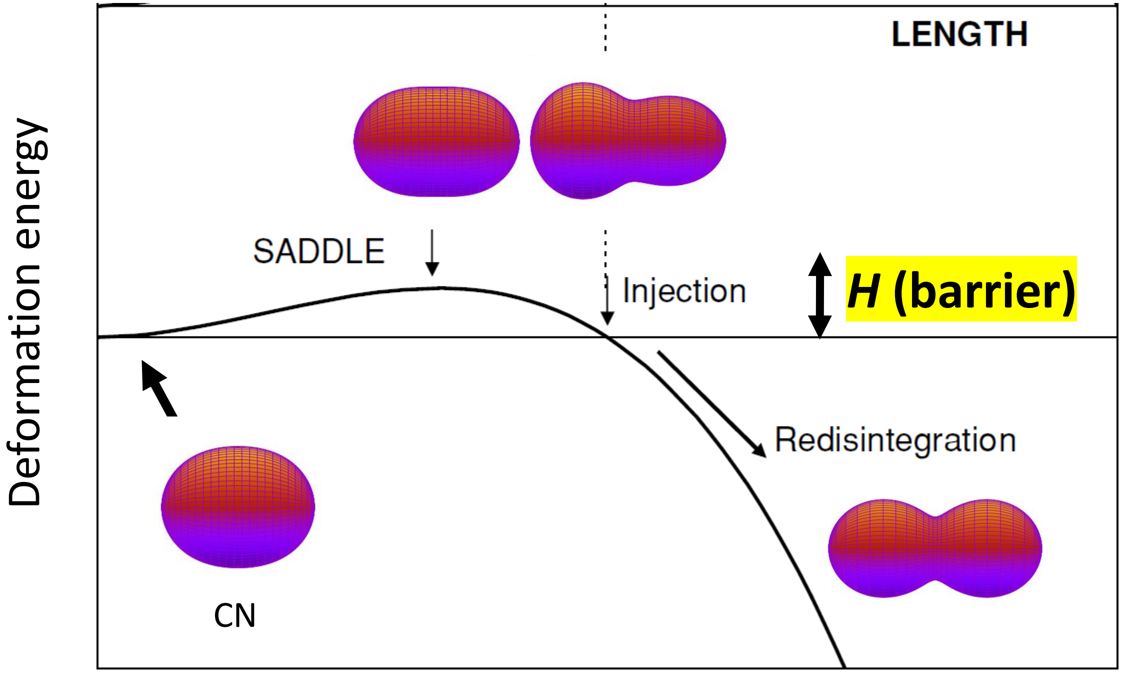

L is the effective elongation (along the fusion path)

Macroscopic deformation energies are calculated using the parameterization of the nuclear shapes by two spheres joined smoothly by a third quadratic surface of revolution.

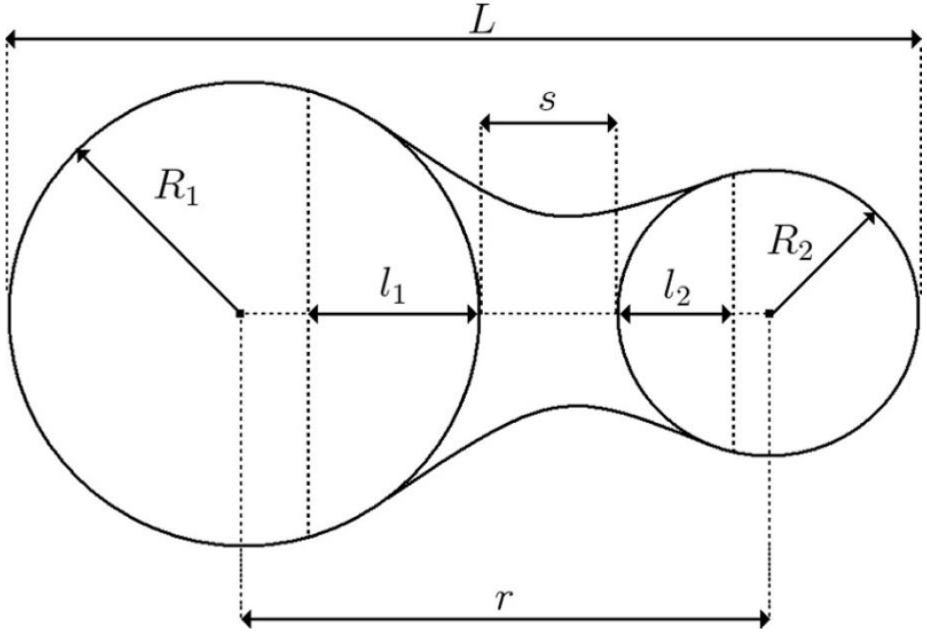

The distance between the nuclear surfaces of two colliding nuclei at the **injection point** s_{inj} is the only adjustable parameter of the model.

s_{inj} distance was parametrized by analyzing 27 cold fusion reactions.

$$s_{inj} = 0.878 \text{ fm} - 0.294 \times (E_{c.m.} - B_0) \text{ fm/MeV}$$

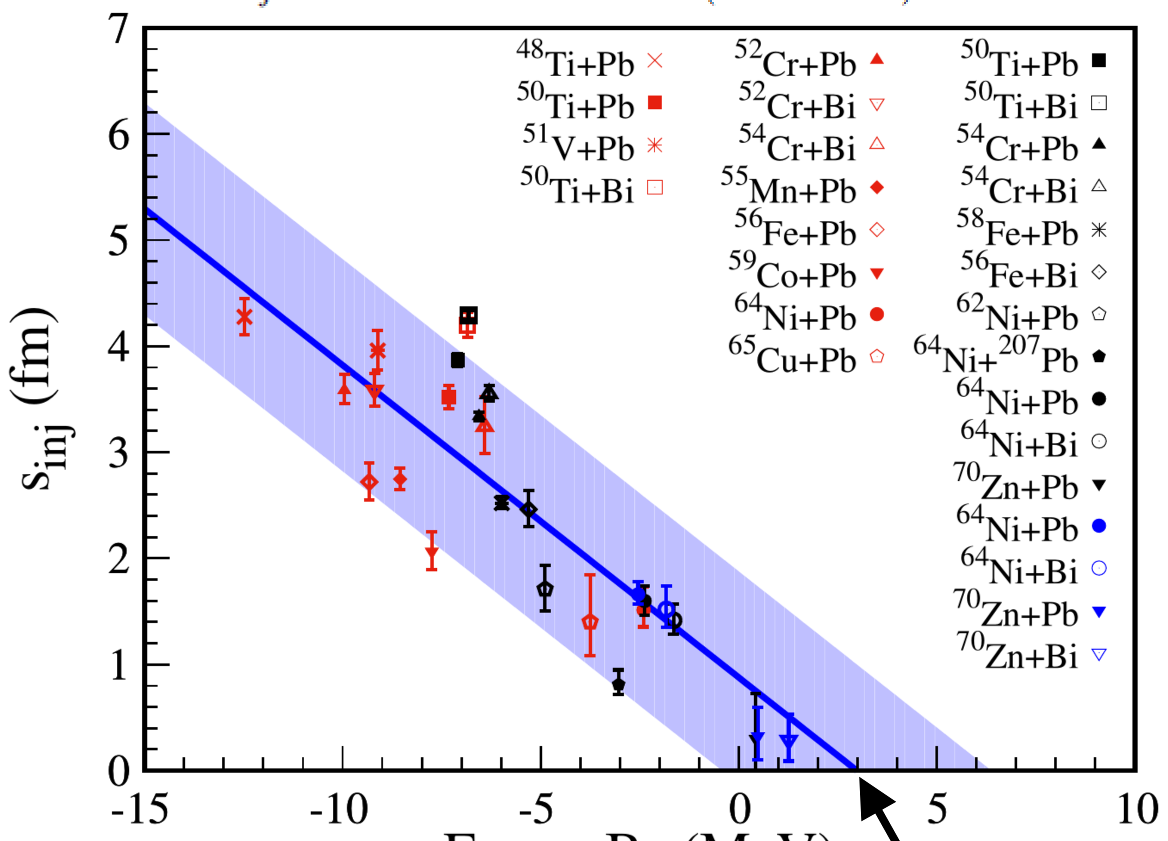

Tangent configuration

Energy relative to the entrance channel barrier B_0

Macroscopic deformation energies are calculated using the parameterization of the nuclear shapes by two spheres joined smoothly by a third quadratic surface of revolution.

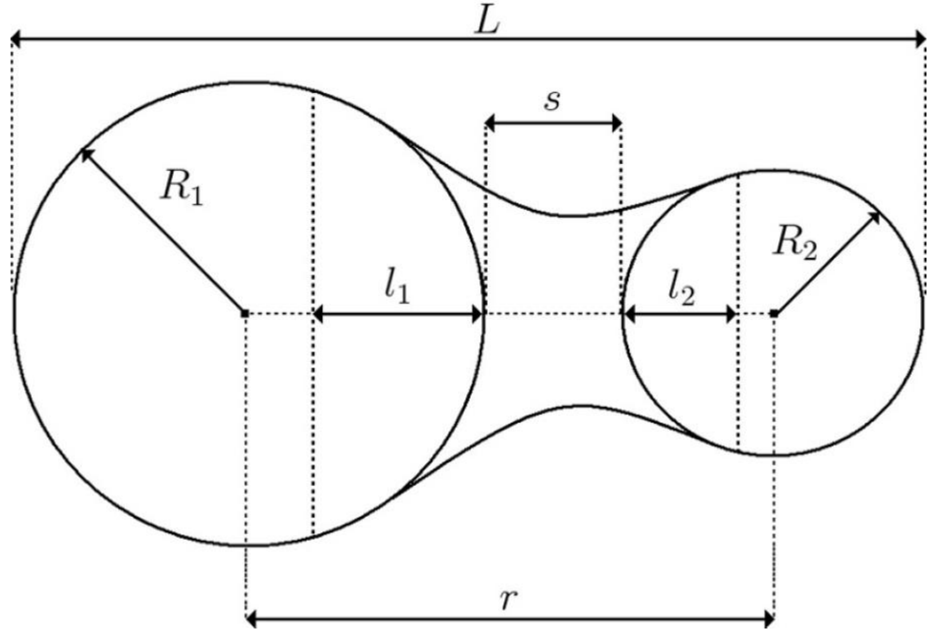

The distance between the nuclear surfaces of two colliding nuclei at the **injection point** s_{inj} is the only adjustable parameter of the model.

s_{inj} distance was parametrized by analyzing 27 cold fusion reactions.

NARODOWE CENTRUM BADAŃ JĄDROWYCH ŚWIERK

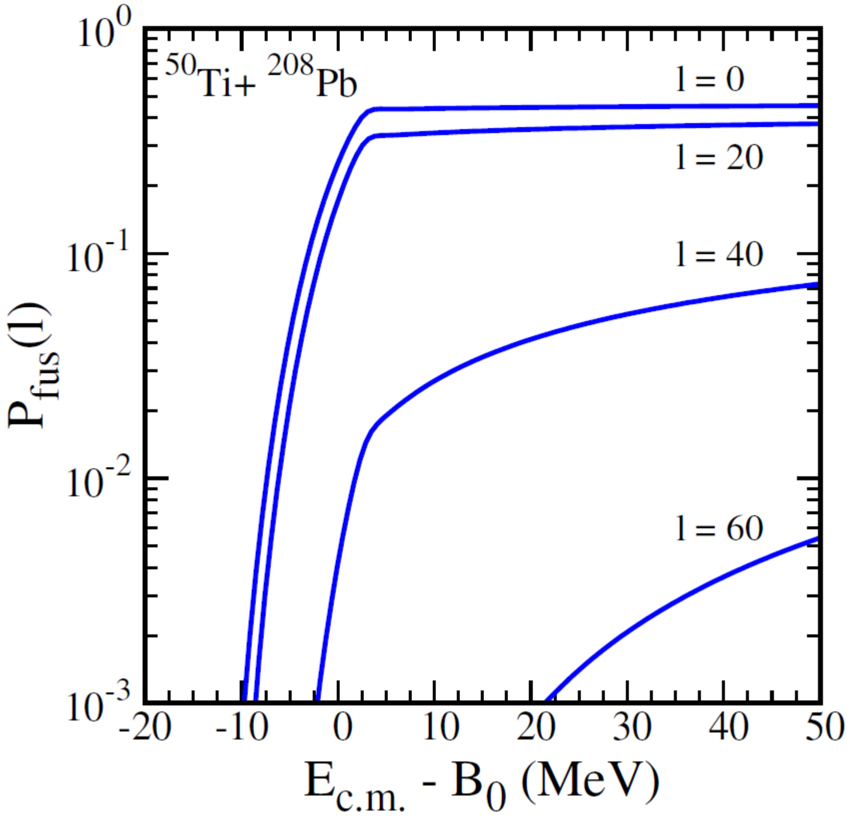

Energy relative to the entrance channel barrier B_0

B_0 = 191.3 MeV

$E^*(E_{c.m.} = B0)$ = 21.7 MeV

l = 0

Central collision

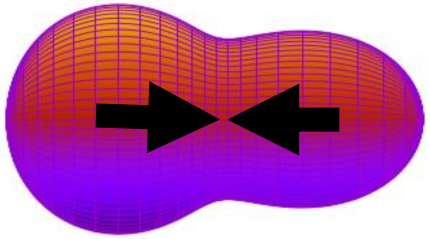

Peripheral collisions

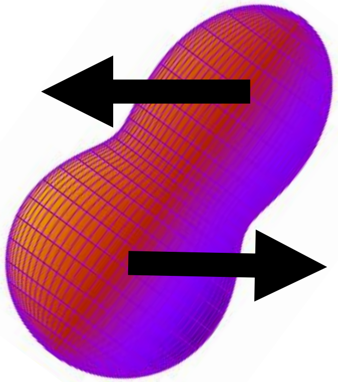

Impact Parameter

Higer partial waves l

=

Higher rotational energy

=

Higher barrier $H(l)$

=

Lower $Pfus(l)$

Fusion probability averaged over l

$$P_{fus}(E_{c.m.}) = \frac{\sum_{l=0}^{lmax}(2l+1)P_{fus}(l)}{(2l_{max}+1)^2}$$

Below *B0*, the *Pfus* growth comes from the reduction in the height of the internal barrier opposing fusion.

$s_{injection}$ > 0 fm

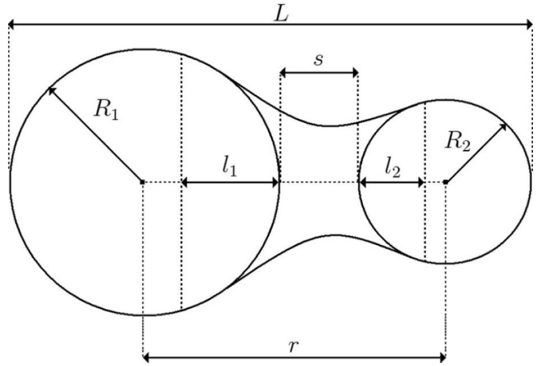

Tangent configuration of projectile and target ($s_{injection}$ = 0 fm)

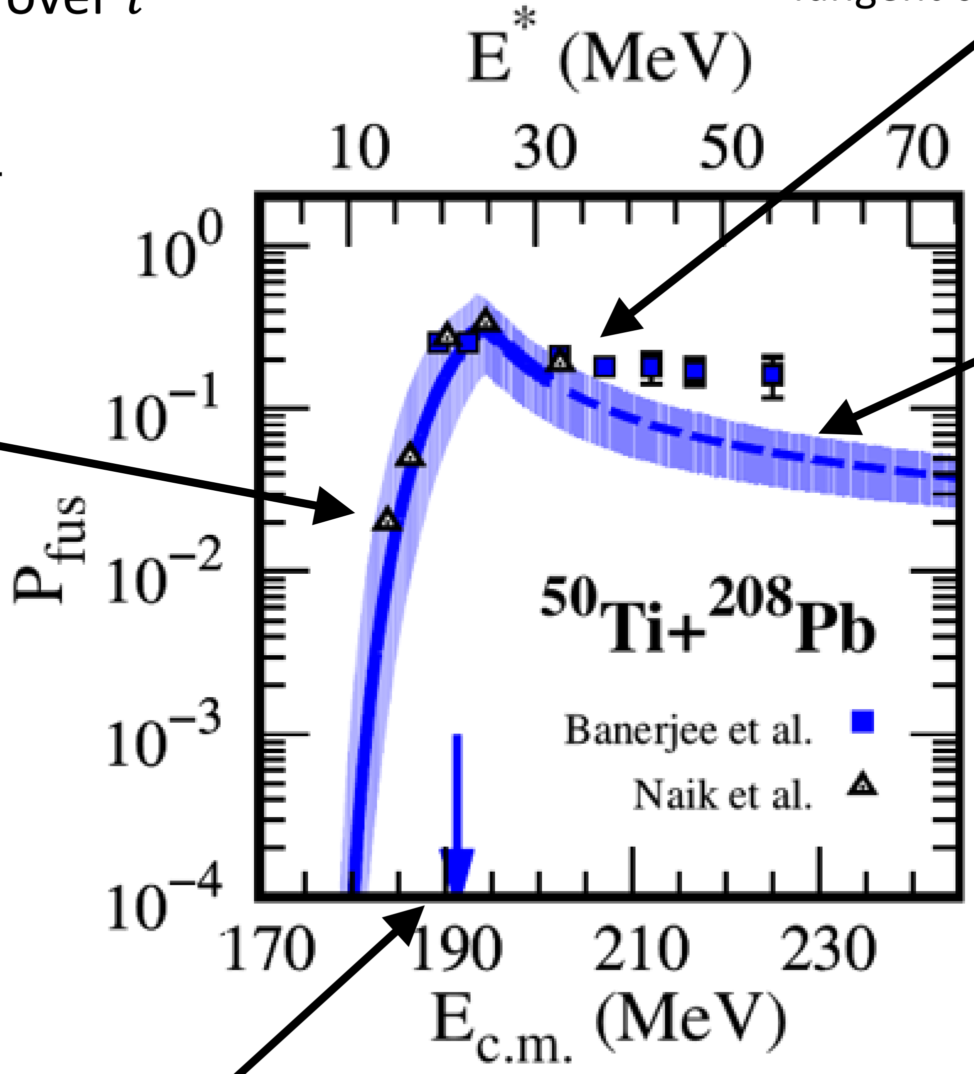

The *Pfus* saturation above *B0* results from suppression of the contributions from higher partial waves and can be linked to the critical angular momentum.

The difference between rotational energies in the fusion saddle and the contact (sticking) configuration plays a major role in CN formation at energies above *B0.*

B0 - entrance channel barrier (Coulomb+Nuclear potential)

NARODOWE CENTRUM BADAŃ JĄDROWYCH ŚWIERK

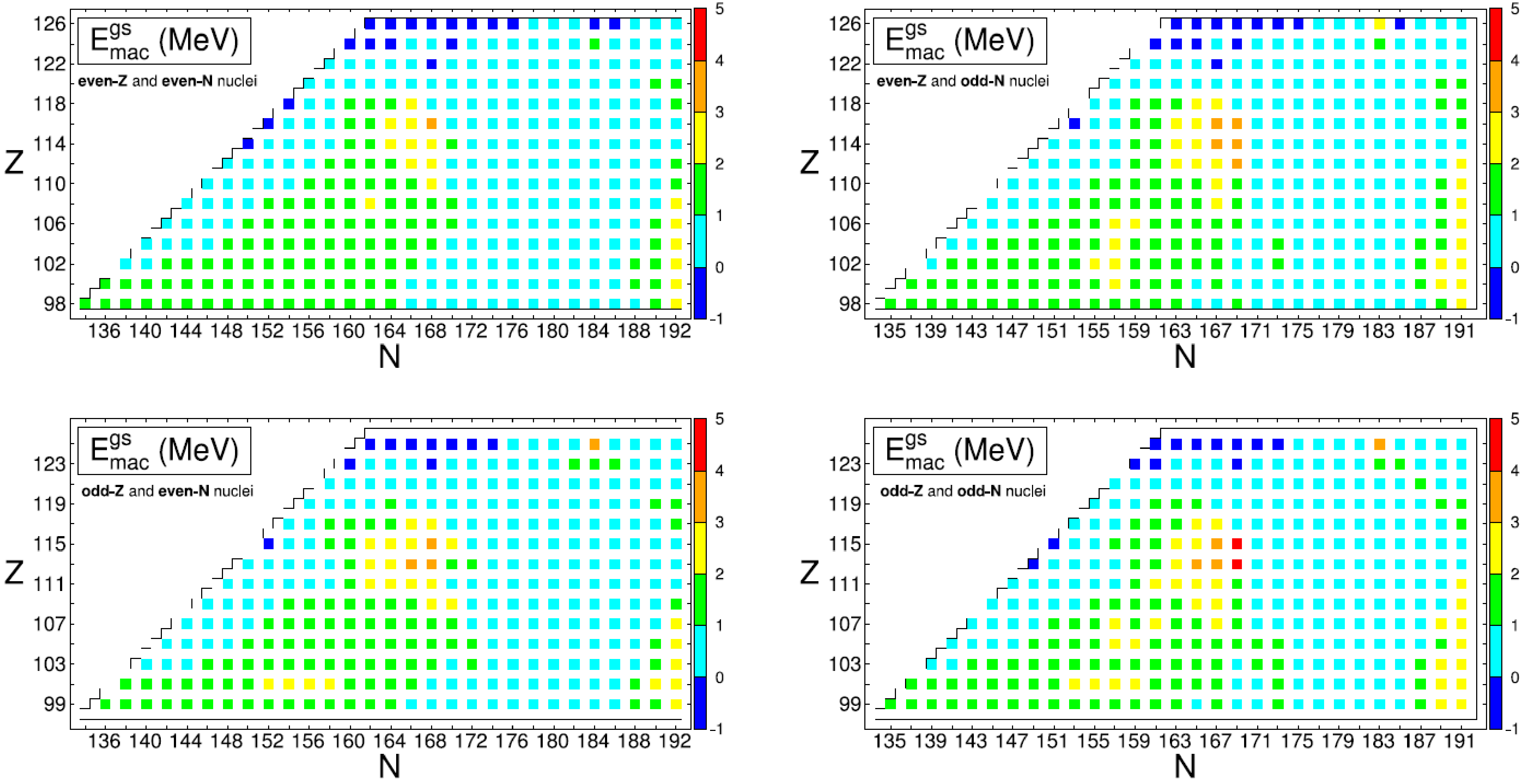

P. Jachimowicz, M. Kowal, J. Skalski, Properties of heaviest nuclei with 98≤Z≤126 and 134≤N≤192, Atomic Data and Nuclear Data Tables, Volume 138, 2021, 101393

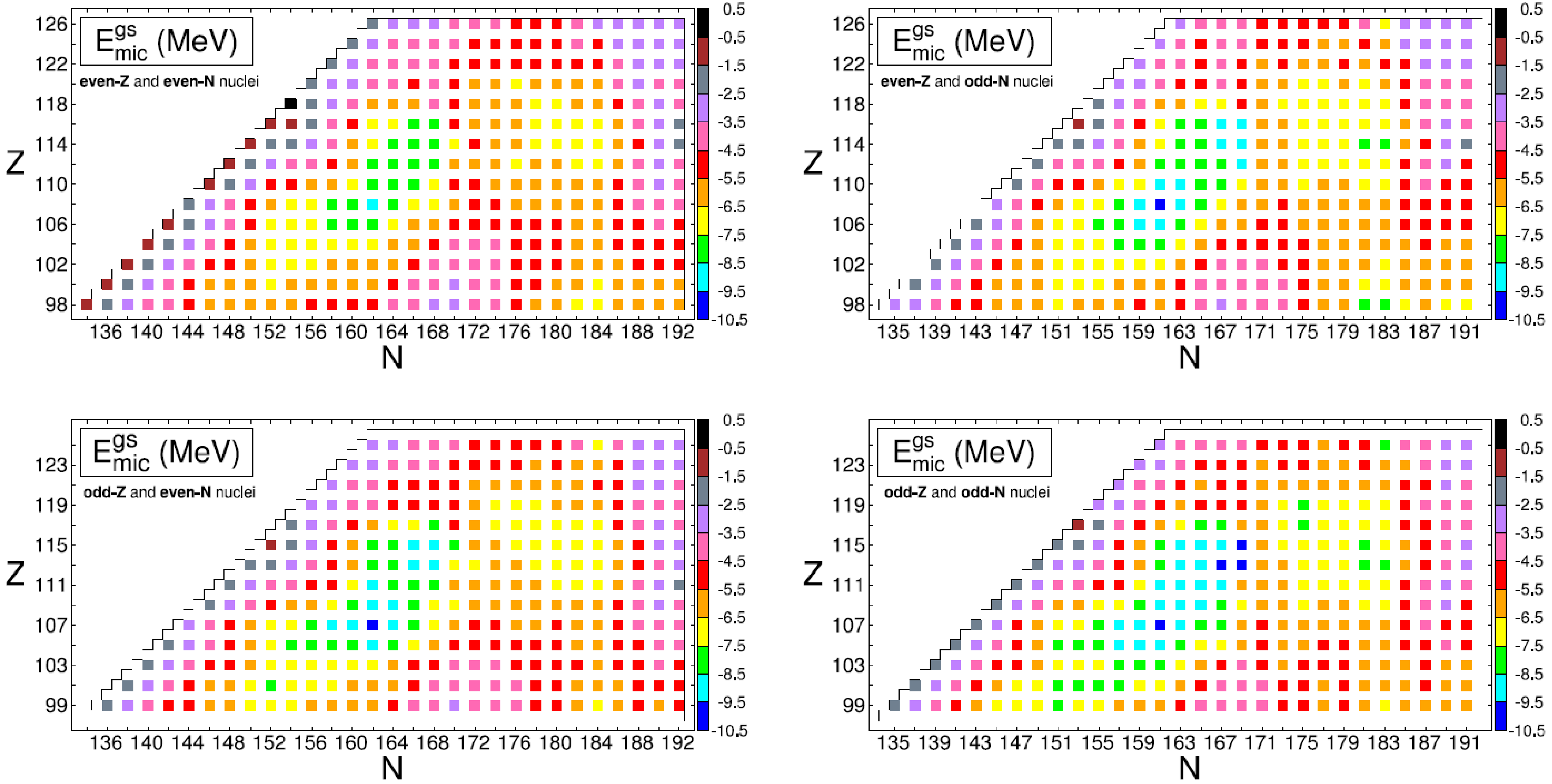

Fig. 2. Calculated microscopic component E^{gs}_{mic} of the ground state binding energy in 4 separate groups of nuclei.

P. Jachimowicz, M. Kowal, J. Skalski, Properties of heaviest nuclei with 98≤Z≤126 and 134≤N≤192, Atomic Data and Nuclear Data Tables, Volume 138, 2021, 101393

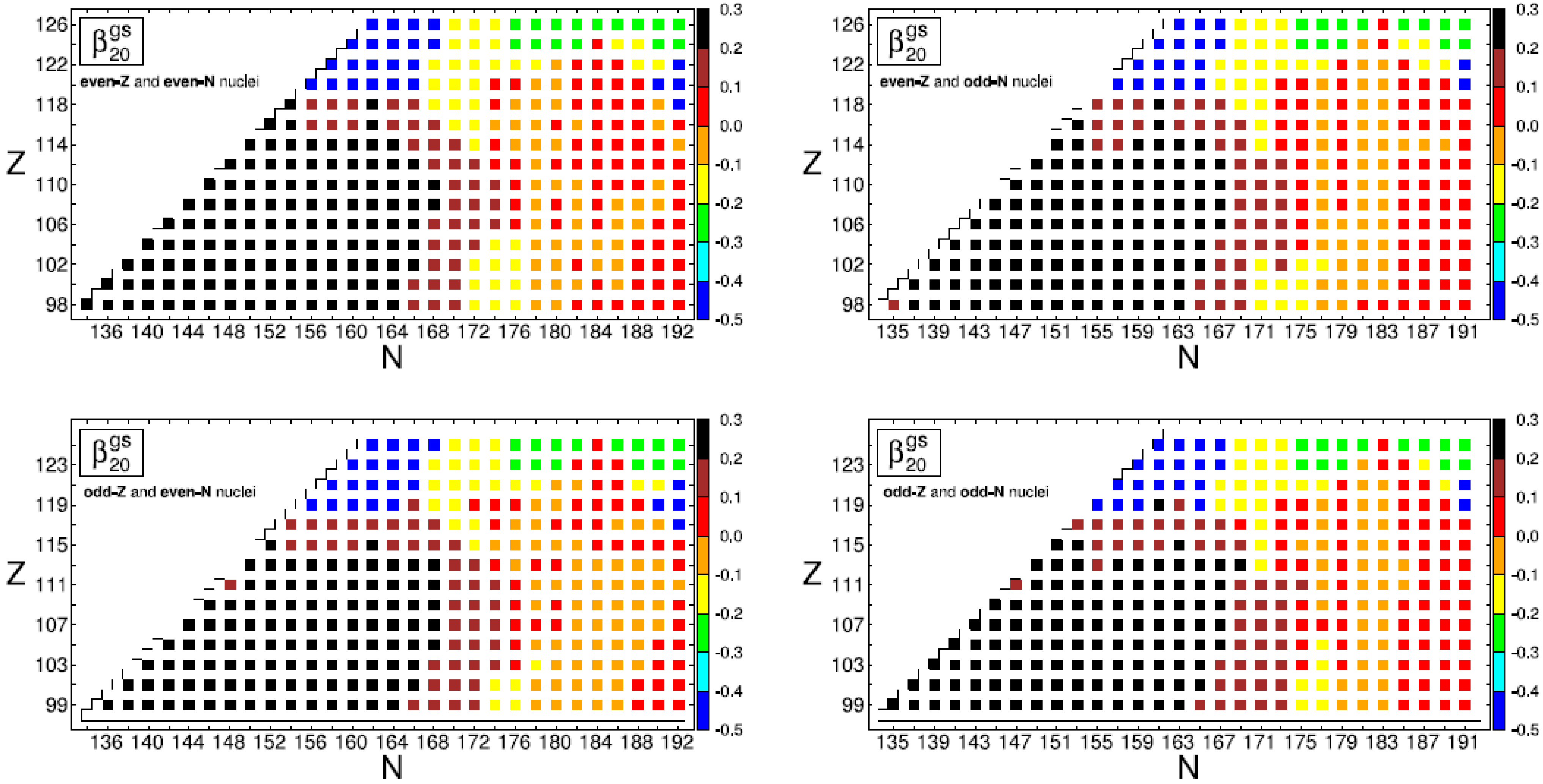

Fig. 4. Calculated ground-state quadrupole deformations β_{20}^{gs} in 4 separate groups of nuclei.

P. Jachimowicz, M. Kowal, J. Skalski, Properties of heaviest nuclei with 98≤Z≤126 and 134≤N≤192, Atomic Data and Nuclear Data Tables, Volume 138, 2021, 101393

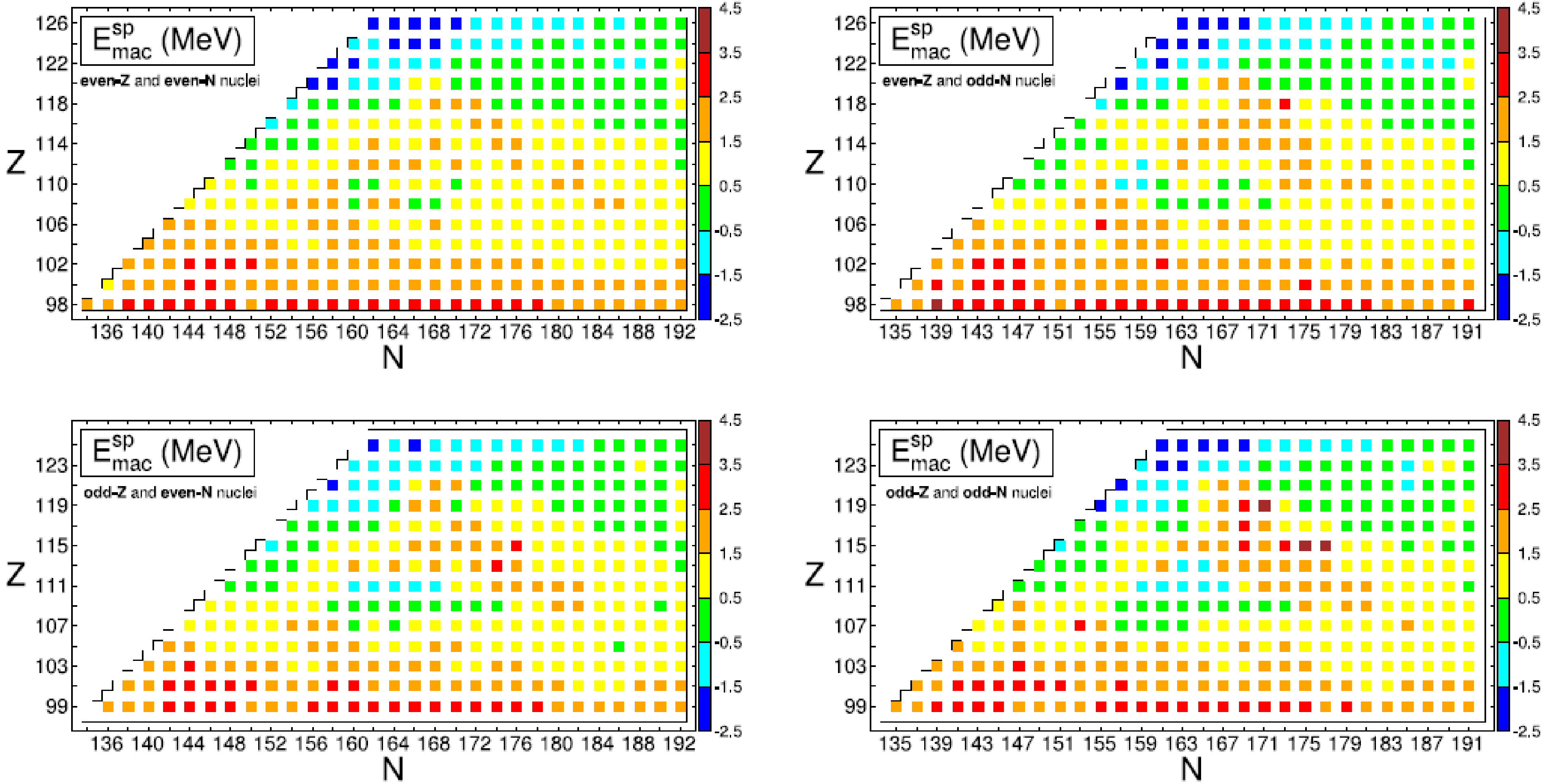

Fig. 12. As in Fig. 1, but for the calculated saddle points.

P. Jachimowicz, M. Kowal, J. Skalski, Properties of heaviest nuclei with 98≤Z≤126 and 134≤N≤192, Atomic Data and Nuclear Data Tables, Volume 138, 2021, 101393

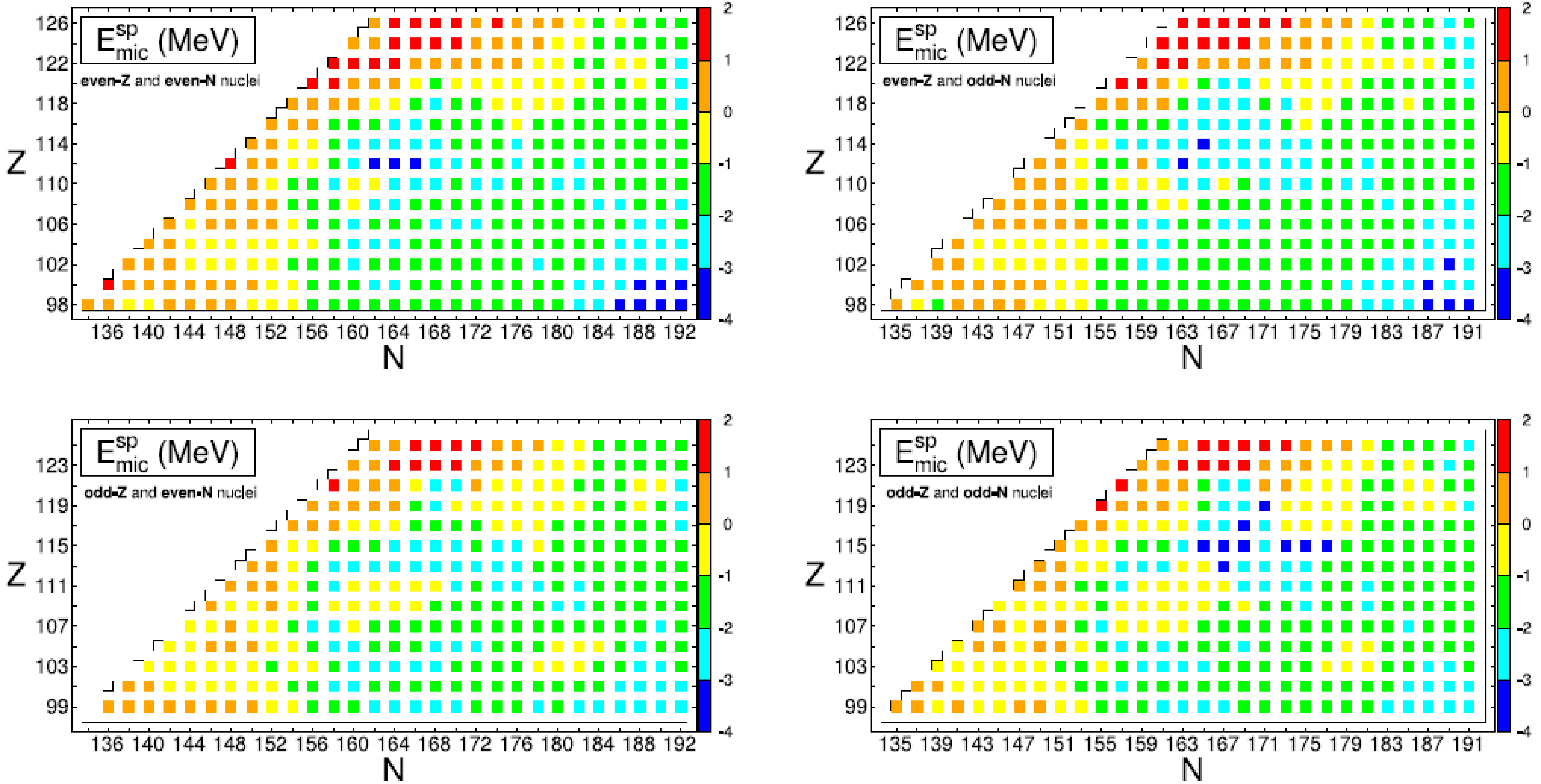

Fig. 13. As in Fig. 2, but for the calculated saddle points.

P. Jachimowicz, M. Kowal, J. Skalski, Properties of heaviest nuclei with 98≤Z≤126 and 134≤N≤192, Atomic Data and Nuclear Data Tables, Volume 138, 2021, 101393

NARODOWE CENTRUM BADAŃ JĄDROWYCH ŚWIERK